Title

Orexinergic bouton density is lower in the cerebral cortex of cetaceans compared to artiodactyls

Authors

Dell, Leigh-Anne
Spocter, Muhammad A
Patzke, Nina
et al.

Publication Date

2015-10-01

DOI

10.1016/j.jchemneu.2015.07.007

Peer reviewed

HHS Public Access

Author manuscript

J Chem Neuroanat. Author manuscript; available in PMC 2021 December 23.

Published in final edited form as:

J Chem Neuroanat. 2015 October ; 68: 61–76. doi:10.1016/j.jchemneu.2015.07.007.

Orexinergic bouton density is lower in the cerebral cortex of cetaceans compared to artiodactyls

Leigh-Anne Dell[a], **Muhammad A. Spocter**[a,b], **Nina Patzke**[a], **Karl Æ. Karlson**[c], **Abdulaziz N. Alagaili**[d,e], **Nigel C. Bennett**[d,f], **Osama B. Muhammed**[d], **Mads F. Bertelsen**[g], **Jerome M. Siegel**[h], **Paul R. Manger**[a,d,*]

[a]School of Anatomical Sciences, Faculty of Health Sciences, University of the Witwatersrand, 7 York Road, Parktown, 2193 Johannesburg, South Africa

[b]Department of Anatomy, Des Moines University, Des Moines, IA 50312, USA

[c]Biomedical Engineering, Reykjavik University, Menntavegur 1, 101 Reykjavik, Iceland

[d]KSU Mammals Research Chair, Department of Zoology, King Saud University, Riyadh 11451, Saudi Arabia

[e]Saudi Wildlife Authority, Riyadh 11575, Saudi Arabia

[f]Department of Zoology and Entomology, University of Pretoria, Pretoria 0002, South Africa

[g]Centre for Zoo and Wild Animal Health, Copenhagen Zoo, Frederiksberg, Denmark

[h]Department of Psychiatry, University of California, Los Angeles, Neurobiology Research 151A3, Sepulveda VAMC, 16111 Plummer Street, North Hills, CA 91343, USA

Abstract

The species of the cetacean and artiodactyl suborders, which constitute the order Cetartiodactyla, exhibit very different sleep phenomenology, with artiodactyls showing typical bihemispheric slow wave and REM sleep, while cetaceans show unihemispheric slow wave sleep and appear to lack REM sleep. The aim of this study was to determine whether cetaceans and artiodactyls have differently organized orexinergic arousal systems by examining the density of orexinergic innervation to the cerebral cortex, as this projection will be involved in various aspects of cortical arousal. This study provides a comparison of orexinergic bouton density in the cerebral cortex of twelve Cetartiodactyla species (ten artiodactyls and two cetaceans) by means of immunohistochemical staining and stereological analysis. It was found that the morphology of the axonal projections of the orexinergic system to the cerebral cortex was similar across all species, as the presence, size and proportion of large and small orexinergic boutons were similar. Despite this, orexinergic bouton density was lower in the cerebral cortex of the cetaceans studied compared

*Corresponding author at: School of Anatomical Sciences, Faculty of Health Sciences, University of the Witwatersrand, 7 York Road, Parktown, 2193 Johannesburg, South Africa. Paul.Manger@wits.ac.za (P.R. Manger).

Ethical statement

The animals used in the present study were caught from wild populations in South Africa, Saudi Arabia, Iceland and Greenland, respectively, under permission and supervision from the appropriate wildlife directorates in both countries. All animals were treated and used according to the guidelines of the University of the Witwatersrand Animal Ethics Committee, which parallel those of the NIH for the care and use of animals in scientific experimentation.

to the artiodactyls studied, even when corrected for brain mass, neuron density, glial density and glial:neuron ratio. Results from correlational and principal component analyses indicate that glial density is a major determinant of the observed differences between artiodactyl and cetacean cortical orexinergic bouton density.

Keywords

Cetartiodactyla; Orexin; Hypocretin; Comparative neuroanatomy; Evolution; Comparative sleep; Mammalia

1. Introduction

Orexin/hypocretin is a neuropeptide synthesized by neurons located within the hypothalamus that give rise to axonal projections found throughout the brain (Horvath et al., 1999). In most mammals the majority of these orexinergic neurons are found within the lateral hypothalamus and perifornical area, but have also been observed in the zona incerta region and the ventrolateral hypothalamus near the optic tract (Peyron et al., 1998; van den Pol, 1999; Wagner et al., 2000; Iqbal et al., 2001; Moore et al., 2001; Yoshida et al., 2006; Nixon and Smale, 2007; Datta and MacLean, 2007; Ettrup et al., 2010; Kruger et al., 2010; Bhagwandin et al., 2011a,b; Gravett et al., 2011; Calvey et al., 2013; Dell et al., 2013; Maseko et al., 2013). A study by Dell et al. (2012) comparing the distribution and number of orexinergic neurons in the brain of the giraffe and harbour porpoise revealed an additional novel medially located parvocellular cluster of orexinergic neurons in the hypothalamus of these two species, which has since also been reported in the African elephant (Maseko et al., 2013). Additionally, for a comparable brain mass, the harbour porpoise had significantly more orexinergic neurons (around 6000) in the hypothalamus than the giraffe, but the giraffe had significantly larger orexinergic neuronal somata (by approximately 1000 μm^3 for both magnocellular and parvocellular neurons) than that of the harbour porpoise. As this parvocellular orexinergic cluster had not been identified in other species, nor had the differences in neuronal numbers and size been reported, Dell et al. (2012) concluded that the orexinergic system is potentially more complex in Cetartiodactyla compared to other mammals. Despite this, it is currently unclear whether these novel findings are associated with differences in the terminal networks of the orexinergic system in these species and if differences do occur, whether they have any functional consequences.

Physiological studies demonstrate that orexinergic neuronal firing patterns are greatest during periods of wakefulness, motor activation and sustained attentiveness to external stimuli and the environment (Datta and MacLean, 2007; Alexandre et al., 2013). Thus, the orexinergic system has been implicated in several functions including the promotion and maintenance of arousal and wakefulness (Alexandre et al., 2013), the regulation of food consumption (Edwards et al., 1999), energy metabolism, thermo-regulation and locomotion (Peyron et al., 1998; Mintz et al., 2001; Spinazzi et al., 2006), with an overall involvement in “work for reward” behaviours, or in the case of humans, for alertness linked to being happy (Mileykovskiy et al., 2005; McGregor et al., 2011; Blouin et al., 2013). While cetaceans and artiodactyls both belong to the order Cetartiodactyla (Price et al., 2005), there are substantial

differences in their life history, all of which appear to be related to functions associated with the orexinergic system. Cetaceans are known to exhibit unihemispheric slow waves and little to no REM sleep (Lyamin et al., 2008), while artiodactyls show the standard bihemispheric mammalian sleep patterns, including REM (Bell and Itabisashi, 1973; Tobler and Schwierin, 1996). Cetacean limbs and necks have been reduced so much that they no longer have a significant locomotor function, whereas in artiodactyls a range of neck and limb proportions are evident (Badlangana et al., 2009). While both groups require substantial food ingestion, cetaceans are carnivorous, whereas the artiodactyls are herbivorous. Cetaceans are under constant, significant thermal pressures due to their aquatic environment (Manger, 2006), whereas the artiodactyls have mechanisms in place to prevent overheating (Kuhnen, 1997; Jessen, 1998, 2001; Mitchell et al., 2002). Additionally, it has been demonstrated that dolphins can continuously maintain vigilant behaviour for at least 15 days without any signs of sleep deprivation (Ridgway et al., 2006, 2009; Branstetter et al., 2012), an observation not made, but unlikely to be present, in artiodactyls.

Given these variations in the life histories, environments and behaviour of the members of the order Cetartiodactyla, these species may provide an important model for understanding the role of orexinergic neurons and their terminal networks (Dell et al., 2012). It has been reported that sustained arousal, vigilance and cognitive function may be mediated via orexinergic projections to the cortex (Bayer et al., 2004; Yamada et al., 2008). Specifically, in the rat prefrontal cortex it has been demonstrated that orexin has a direct excitatory postsynaptic effect on pyramidal neurons (Song et al., 2006; Yan et al., 2012). Thus, the density of orexin boutons in the cerebral cortex may provide an indication of the degree to which orexin innervation modulates the activity of cortical neurons to support the behaviours associated with activation of hypothalamic orexinergic neurons. Given the higher number of orexinergic neurons in the harbour porpoise hypothalamus when compared to the giraffe hypothalamus (Dell et al., 2012), it is possible that cetaceans as a whole have an increased bouton density in the cerebral cortex when compared to artiodactyls; however, this possibility needs to be balanced with the observation that the orexinergic neurons in the giraffe are larger than those in harbour porpoise, and thus may support larger and more branched axons than the cetaceans in general, leading to a higher orexin bouton density in the artiodactyl cerebral cortex in general. In order to determine which of these possibilities, if either, occurs, the current study provides a comparison of orexinergic bouton density in the anterior cingulate and occipital cerebral cortex of a number of Cetartiodactyl species by means of immunohistochemical staining and stereological analysis.

2. Materials and methods

2.1. Specimens

The current study examined orexinergic boutons in the cerebral cortex of 12 individuals representing 12 Cetartiodactyl species. The brains of ten individuals from 10 artiodactyl species [Arabian oryx (*Oryx leucoryx*), springbok (*Antidorcas marsupialis*), nyala (*Tragelaphus angasii*), blue wildebeest (*Connochaetes taurinus*), domestic pig (*Sus scrofa*), African buffalo (*Syncerus caffer*), giraffe (*Giraffa camelopardalis*), dromedary camel (*Camelus dromedarius*), Nubian ibex (*Capra nubiana*) and river hippopotamus

(*Hippopotamus amphibius*)] were obtained from South Africa, Saudi Arabia and Denmark under appropriate governmental permissions. The brains of one individual from the two species of cetaceans [harbour porpoise (*Phocoena phocoena*) and northern minke whale (*Balaenoptera acutorostratus*)] were obtained from Greenland and Iceland respectively, under appropriate governmental permissions. All animals were males and based on body mass, dental and genital maturity were all adults of reproductive age. The animals were treated according to the guidelines of the University of Witwatersrand Animal Ethics Committee, which parallel those of the NIH for care and use of animals in scientific experimentation. Within 30 min of euthanasia, the head of each artiodactyl was perfused through the carotid arteries initially with a rinse of 1 l of 0.9% saline per 2 kg of body tissue, followed by fixation with 1 l of 4% paraformaldehyde in 0.1 M phosphate buffer (PB) per 1 kg body tissue (Manger et al., 2009). For the cetaceans, the harbour porpoise was perfused via the heart, within 30 min of death, using the above mentioned ratios of saline and 4% paraformaldehyde, whereas the brain of the Northern minke whale was immersion fixed in 4% paraformaldehyde in 0.1 M phosphate buffer within 30 min of death. The brains were removed from the skull and post-fixed (4% paraformaldehyde in 0.1 M PB) for 72 h at 4 °C. Thereafter, the brains were transferred to a solution of 30% sucrose in 0.1 M PB at 4 °C until they had equilibrated and were then transferred to an antifreeze solution containing 30% glycerol, 30% ethylene glycol, 30% distilled water and 10% 0.244 M PB. Once again, the brains were allowed to equilibrate in the solution at 4 °C and were then moved to a −20 °C freezer for storage until sectioning.

2.2. Tissue selection and immunohistochemical staining

Blocks of cortical tissue from the occipital cortex (putative primary visual cortex, V1, based on summaries of cortical organization for artiodactyls and cetaceans provided in Johnson, 1990; Manger, 2006) and the anterior cingulate cortex (taken immediately above the rostrum of the corpus callosum, AC) were dissected from each brain. These regions were chosen for two reasons, first, they can be relatively reliably identified across the species studied making for comparisons of putatively homologous cortical areas across species, and second, as they represent a primary sensory processing area and a cortical region involved in higher order processing, allowing us to determine whether there is significant regional variation in orexinergic innervation of the cerebral cortex. These tissue blocks were placed in 30% sucrose in 0.1 M PB at 4 °C until they had equilibrated. The tissue blocks were then frozen in crushed dry ice and mounted onto an aluminium stage that was attached to a sliding microtome. All tissue blocks were sectioned in the coronal plane, with a section thickness of 50 μm. A one in two series was stained for Nissl substance (with cresyl violet) and orexin (with an antibody directed against Orexin-A). Nissl sections were mounted on 0.5% gelatine coated glass slides and then cleared in a solution of 1:1 chloroform and methanol overnight, after which the sections were stained with 1% cresyl violet. The sections used for immunohistochemistry were initially treated for 30 min with an endogenous peroxidase inhibitor (49.2% methanol: 49.2% 0.1 M PB: 1.6% of 30% H_2O_2), followed by three 10 min rinses in 0.1 M PB. The sections were then pre-incubated at room temperature for 2 h in a blocking buffer solution containing 3% normal serum (NGS, Chemicon/Millipore), 2% bovine serum albumin (BSA, Sigma) and 0.25% Triton X-100 (Merck) in 0.1 M PB. The sections were then placed in a

primary antibody solution (blocking buffer with correctly diluted primary antibody) and incubated at 4 °C for 48 hours under gentle shaking. To reveal orexinergic cortical boutons, an anti-orexin-A antibody (AB3704, Chemicon/Millipore, raised in rabbit) was used at a dilution of 1:3000. The immunogen of this antibody is a synthetic peptide from bovine orexin-A raised against amino acids 14–33 (CRLYELLHGAGN-HAAGILTL-amide) of the N-terminus of the molecule (Sakurai et al., 1998; Nambu et al., 1999) and provided similar staining to that reported previously in the laboratory rat (Nambu et al., 1999). This was followed by three 10 min rinses in 0.1 M PB, after which the sections were incubated in a secondary antibody solution for two hours at room temperature. The secondary antibody solution contained a 1:1000 dilution of biotinylated anti-rabbit IgG (BA-1000, Vector Labs) in a blocking buffer solution containing 3% NGS and 2% BSA in 0.1 M PB. This was followed by three 10 min rinses in 0.1 M PB after which the sections were incubated in AB solution (Vector Labs) for 1 h. After three further 10 min rinses in 0.1 M PB, the sections were placed in a solution of 0.05% diaminobenzidine (DAB) in 0.1 M PB for five minutes (1 ml/section), followed by the addition of 3 μl of 30% H_2O_2 to each 1 ml of solution in which each section was immersed. Chromatic precipitation of the sections was monitored visually under a low power stereomicroscope. The precipitation process was stopped by immersing the sections in 0.1 M PB and then rinsing them twice more in 0.1 M PB. Omission of the primary or secondary antibody in selected sections was employed as controls for the immunohistochemical protocol, for which no staining was evident. The immunohistochemically stained sections were mounted on 0.5% gelatine coated slides and left to dry overnight. The sections were then dehydrated in a graded series of alcohols, cleared in xylene and cover slipped with Depex.

2.3. Stereological analysis

Using a design-based stereological approach we estimated the density of neurons, glia and orexinergic immunopositive boutons (OxA+) in the grey matter of the occipital cortex and the anterior cingulate cortex (e.g., Schenker et al., 2010; Thannickal et al., 2007). An Olympus BX-60 light microscope equipped with a motorized stage, digital camera and integrated StereoInvestigator software (MBF Bioscience, Williston, VT, USA, version 8) was used for the stereological counts.

Neuronal and glia densities were estimated from Nissl-stained sections (Fig. 1) using the optical fractionator method (West et al., 1991). A pilot study was used to determine the optimal sampling parameters and grid dimensions to place dissector frames in a systematic-random manner. Counting frames and sampling grid sizes were optimized to achieve a mean coefficient of error of 10% or less (Gundersen and Jensen, 1987) [counting frame = 80 μm × 80 μm; sampling grid = 1050 μm × 1050 μm; dissector height = 7 μm], while a guard zone of 2 μm was employed during counting to avoid introduction of errors due to sectioning artefacts (West et al., 1991). Section thickness was measured at every fifth sampling site and neuronal and glial cells were counted in layers II to VI according to the principles of the optical fractionator method (West et al., 1991). The calculated coefficients of error (Schmitz and Hof, 2000) were within the range of ≤0.10 for each cortical area in each specimen and neuron and glial densities were calculated as the ratio of total neuron number over sampled cortical area volume (Table 1).

A pilot study aimed at optimizing the parameters for OxA+ bouton counts indicated that a standard stereological approach would not be appropriate given the heterogeneous distribution of the boutons. To facilitate comparison, we used a modified unbiased stereological approach by performing exhaustive total counts across a standardized 1500 μm region of interest, spanning all six cortical layers (Horvath et al., 1999). The 'optical rotator probe' was used to estimate the mean cross-sectional area of the orexinergic immunopositive boutons and was used in conjunction with fractionator sampling (Gundersen et al., 1988) (Table 2). It was observed across all species that two distinct classes of orexinergic boutons could be seen under high power magnification. Boutons were thus classified as belonging either to the "large" or "small" size classes after examination under 40x magnification. A total of approximately 100–150 boutons per cortical area were counted in each animal and the number of boutons belonging to either of these size classes was expressed as a percentage of the total boutons examined. For further quantification the diameter (i.e., the longitudinal length coincident with the direction of passage of the axons) of 40 randomly selected boutons for each of the two size classes was measured at 100x (oil immersion) using an Axioskop 2 plus microscope equipped with an AxioCam HRc3 camera and Zen lite 2011 software programme.

2.4. Statistical analysis

All statistical analyses were performed using SPSS Statistical Package (Version 22.0). Means were reported for estimates of bouton size as well as numbers of glial cells and neurons, and bivariate Pearson correlation coefficients were derived using the data for brain mass, neuron density, glial density, bouton density and glia:neuron ratio. For the purposes of statistical analysis, we used analysis of variance (ANOVA) to evaluate significant differences between species, using Group (i.e. Artiodactyl or Cetacean) and Brain Region (i.e., anterior cingulate cortex or occipital cortex) as the fixed variables, while neuron density, glial density, glia:neuron ratio and bouton density were entered as dependent variables. Significance levels were tested at $\alpha = 0.05$ and confidence intervals at 95% with Bonferroni adjustment. To further evaluate potential differences between species, we used principal component analysis (PCA) to generate latent variables (principal components) that were uncorrelated with one another. The first principal component explaining the greatest source of variation in the dataset was generated from a linear combination of the following original variables: brain mass; neuron density, glial density, bouton density and glia:neuron ratio. The second principal component explained the remaining source of variation and thus only principal component one and two are reported, as these explained the greatest total proportion of variance in the dataset.

3. Results

Orexinergic immunopositive boutons in the anterior cingulate cortex (AC) and occipital cortex (OC, putative primary visual cortex) of twelve Cetartiodactyla species were visualized by means of immunohistochemistry (Figs. 2 and 3). In all species numerous orexin-A immunoreactive boutons (OxA+) were found scattered across all layers of the cortical grey matter of the AC and OC, and in certain artiodactyl species axonal fibres containing boutons could be seen running from the white matter into layer VI. These

orexinergic boutons could be readily distinguished into large and small boutons (Fig. 4), with the number of small boutons outnumbering the number of large boutons. The mean bouton sizes across the AC and OC appeared fairly homogenous across all Cetartiodactyla, but both bouton and neuron density were always lower in the cetaceans than the artiodactyls. In contrast, the cetaceans had a significantly higher glial density in the OC ($F = 5.764$; $P = 0.026$) and a significantly larger glia:neuron ratio in both the AC and OC compared to artiodactyls ($F = 11.727$, $P = 0.003$) (Table 3). The description provided below applies to both the AC and OC in all species unless otherwise stated.

3.1. Bouton appearance and size

Terminal axonal ramifications with distinct orexinergic boutons were observed to traverse the entire depth of the cortical grey matter in all species examined (Figs. 2 and 3). Although the axons appeared to have no distinct spatial organization, most passed vertically through the layers of the cortex, with a few axons demonstrating a horizontal orientation within a specific cortical layer. The orexinergic boutons were tightly packed along the length of the terminal axons, but the boutons could be readily distinguished due to the larger size of the boutons compared with the axonal diameter (Fig. 4). In addition to this, visual inspection indicated that both large and small orexinergic boutons were located on the same axonal ramification (Fig. 4). In the AC of all species the larger orexinergic boutons appeared more ovoid shaped than the smaller boutons and were scattered along the axonal length (Fig. 2). In contrast, the smaller orexinergic boutons were more spherical in shape and evinced a more clustered distribution along the axon. The distribution and shape of boutons along the axons within the OC of all species was similar to that observed in the AC (Fig. 3).

Large and small orexinergic boutons were evident under visual inspection and thus the boutons were classified as either large or small. Bouton size was quantified by measuring the diameter. Across the AC and OC of all species, small boutons were observed to have a diameter of less than 1.4 μm whereas large boutons had a diameter of greater than 1.4 μm (Table 4, Fig. 5). The overall range for the diameter of the small boutons was 0.419–1.398 μm in both the AC and OC across all species. The overall range for the diameter of the large boutons was 1.406–4.402 μm in the AC and 1.406–4.506 μm in the OC (Table 4, Fig. 5). The average small bouton size across the AC of all species studied was 1.052 μm. The mean OC small bouton size across all species studied was 0.986 μm, being slightly smaller than that observed when compared to the small boutons in the AC. Despite slight variations in average bouton sizes and bouton size ranges, no statistically significant difference between species and cortical areas were observed for the size of the small boutons, nor were any statistically significant correlations between bouton sizes and brain mass, neuronal density, glia density or glia:neuron ratios observed for the small orexinergic boutons ($P > 0.05$; see Tables 5 and 6). The mean AC large bouton size for all species studied was 2.263 μm, while the mean OC large bouton size was 2.333 μm, being slightly larger than that observed for the AC large boutons. Despite slight variations in average bouton sizes and bouton size ranges, no statistically significant differences between species and cortical areas were observed for the size of the large boutons, nor were any statistically significant correlations between bouton sizes and brain mass, neuronal density, glia density or glia:neuron ratios observed for the large orexinergic boutons ($P > 0.05$; see Tables 5 and 6).

3.2. Proportions of large and small orexinergic boutons

There were noticeably more small boutons than large boutons in both the AC and OC of all species studied (Table 4, Figs. 4 and 6). In both the AC and OC of all species examined, the percentage of large boutons ranged from 23–42% and 24–43%, respectively (Fig. 6A). The percentage of small boutons in the AC and OC of all species studied ranged between 58–77% and 57–76%, respectively (Table 4, Fig. 6B). Despite variations in average bouton proportions, no statistically significant difference between species and cortical areas were observed for the proportions of both the large and small boutons, nor were any statistically significant correlations between bouton proportions and brain mass, neuronal density, glia density or glia:neuron ratios observed for both the large and small orexinergic boutons ($P > 0.05$; see Tables 7 and 8).

3.3. Neuronal density in the anterior cingulate and occipital cortex

Within the AC the giraffe, blue wildebeest and domestic pig had the highest neuronal densities of 23 303/mm^3, 22 108/mm^3 and 18 355/mm^3, respectively (Table 4, Fig. 7). Species with the lowest AC neuronal densities included the nyala, minke whale and river hippopotamus with respective neuronal densities of 9432/mm^3, 8671/mm^3 and 7516/mm^3 (Table 4, Fig. 7). Within the OC the domestic pig, blue wildebeest and harbour porpoise had the highest neuronal densities of 23 808/mm^3, 22 957/mm^3 and 20 129/mm^3, respectively (Table 4, Fig. 7), while the dromedary camel and river hippopotamus had substantially lower neuronal densities of 9930/mm^3 and 8135/mm^3, respectively (Table 4; Fig. 7). While for the most part, the species showed relatively little difference in neuronal density between the two cortical regions examined, the domestic pig and harbour porpoise had substantially higher neuronal densities in OC compared to AC, while the dromedary camel and giraffe had substantially higher neuronal densities in AC compared to OC (Fig. 7). No statistically significant correlation between neuronal density and brain mass was observed for either the AC or OC ($P > 0.05$; see Table 3).

3.3.1. Glial density—Glial densities in both cortical areas of all species were substantial, and for the most part were similar between the two cortical areas (Fig. 7). The domestic pig, nyala, river hippopotamus and both cetaceans had substantially higher glial densities in OC compared to AC, while the dromedary camel and giraffe both had higher glial densities in the AC compared to the OC (Fig. 7). The domestic pig, giraffe and African buffalo had the highest glial densities of the artiodactyls, with densities of 1 332 883/mm^3, 107 502/mm^3 and 111 595/mm^3, respectively, while the nyala and river hippopotamus produced the lowest glial densities of 65 040/mm^3 and 58 984/mm^3 (Table 4, Fig. 7); however, the highest glial density sampled was found in the OC of the harbour porpoise (153 415/mm^3) and both cetaceans species had glial densities markedly larger than that observed in the artiodactyls. These observations were confirmed by statistical analyses with an analysis of variance revealing a significant difference in mean glial density between the artiodactyl and cetacean groups ($F = 5.764$; $P = 0.026$) with cetaceans having significantly higher glial densities than the artiodactyls.

3.3.2. Glial:neuron ratio—The glia:neuron ratios were similar across cortical areas investigated within each species (Table 4, Fig. 7); however, when looking between

species, the glia:neuron ratio varied markedly, with the blue wildebeest and giraffe both demonstrating low ratios, while both cetaceans and the river hippopotamus exhibited ratios occupying the higher end of the range observed (Fig. 7). While there appeared to be a trend towards a larger glia:neuron ratio with increasing brain size (i.e., more glia per neuron), this trend was not statistically significant for either anterior cingulate cortex ($r^2 = 0.54$; $P = 0.07$) or occipital cortex ($r^2 = 0.57$; $P = 0.055$), although this was approaching significance in occipital cortex.

3.3.3. Orexinergic bouton density—In all species examined, except for the domestic pig, the density of orexinergic boutons in the AC was higher than the OC (Table 4, Fig. 7). In the domestic pig and the two cetacean species, the density of orexinergic boutons in both regions of cortex examined was quite similar, but in the remaining Artiodactyls, the orexinergic bouton density was significantly higher ($F = 6.269$; $P = 0.021$) in AC compared to OC (Fig. 7). For the most part, in both AC and OC substantially lower orexinergic bouton densities were observed in the cetaceans in comparison to the artiodactyls, although the densities of orexinergic boutons found in the OC of the springbok, blue wildebeest, African buffalo, dromedary camel, nyala and giraffe were similar to that seen in the cetaceans (Fig. 7). The cetaceans, in general, thus appear to have substantially lower orexinergic innervation of the cerebral cortex compared to the closely related artiodactyls.

3.3.4. Orexinergic bouton density in relation to brain mass, neuronal density, glial density and the glia:neuron ratio—When comparing the potential relationships between orexinergic bouton density and brain mass in the artiodactyls, a weak trend of increasing bouton density with increasing brain mass was observed in the AC, while a weak trend of decreasing bouton density with increasing brain mass was observed in OC (Fig. 8). 95% confidence ellipses, based on the artiodactyl data, indicated that within the AC and OC the cetaceans have lower bouton densities than you would predict for their brain mass. Thus, it would appear that for their brain mass, the cetaceans generally have lower orexinergic bouton densities than you would predict based on the artiodactyl data. When comparing orexinergic bouton density to neuronal density, glia density and glia:neuron ratio in the artiodactyls, in both the AC and OC no relationship between the two parameters was evident (Fig. 8) ($P > 0.05$). In all comparisons, the orexinergic bouton densities in cetaceans were lower than those observed in artiodactyls.

Using principal component analysis we reduced the five variables (brain mass, neuron density, glia density, glia:neuron ratio and bouton density) into two composite variables (principal components) that best describe the variation in the sample. The principal components that described the highest amount of variance in the sample were PC1 and PC2 both of which had eigenvalues greater than 1. PC1 explained 97% of the variance and PC2 explained 2.7% of the total variance in the sample. The scores plot (Fig. 9A) indicates a clear separation of the species into two major clusters, corresponding to what is known about the phylogenetic relationship of these species. Notably, the minke whale and harbour porpoise are isolated in one quadrant apart from the artiodactyls forming a discrete cetacean cluster, although this analysis proved insufficient in distinguishing cetaceans from the buffalo and pig, both of which have higher glial densities and PC1 values. Based on

the factor-loading plot (Fig. 9B), glia density was the most useful variable in describing the first principal component (i.e., factor loading ≥ 0.70) and in helping to drive the statistical separation between the data points. Although this is a statistical finding and not an explanation in mechanistic terms, these results echo the pattern observed in the analysis of variance indicating that cetaceans differ significantly from artiodactyls in the mean glial density, glial:neuron ratio and bouton density. Cumulatively, these series of quantitative approaches point to the fact that cetaceans differ significantly from artiodactyls in the arrangement of the orexinergic terminal networks in the anterior cingulate and occipital cortices.

4. Discussion

The current study provides the first detailed qualitative and quantitative analysis of the appearance and density of orexinergic terminal networks in two regions of the cerebral cortex of several artiodactyl and two cetacean species. The current work was initiated by earlier findings that: (1) giraffes and harbour porpoises shared a novel parvocellular cluster of orexinergic neurons in the hypothalamus; (2) the harbour porpoises appear to have a greater number of orexinergic neurons than giraffes with a similar brain mass; (3) the orexinergic neurons of the giraffes are larger than those of the habrour porpoise; and (4) the cetaceans exhibit an unusual form of mammalian sleep (Lyamin et al., 2008; Dell et al., 2012). Due to these differences, it was hypothesized that the orexinergic terminal networks in the cerebral cortex would differ between cetaceans and artiodactyls, but it was unclear what differences might be found (Dell et al., 2012). Our findings indicate that there are a lot of similarities in the structure of the orexinergic terminal networks in the cetaceans and artiodactyls studied, sharing features such as large and small boutons that are similar in both size and proportions irrespective of brain size or phylogenetic affinity within the Cetartiodactyla. Despite this, the clearest finding is that the density of the orexinergic boutons in the cerebral cortex, when compared against brain mass, neuron density, glia density and glia:neuron ratio, is significantly lower in the cetaceans studied than the artiodactyls studied, including the river hippopotamus which is the closest extant relative of the cetaceans. Principal components analysis indicated that the density of glia within the cerebral cortex is the major factor correlating with the difference in orexinergic bouton density between the cetaceans and artiodactyls studied.

4.1. Evolutionarily conservative aspects of the orexinergic system

The orexinergic system within the mammalian brain shows a great deal of anatomical similarity across a wide range of mammalian species in which this system has been previously studied. For example, the orexinergic cells within the hypothalamus can generally be divided into three magnocellular clusters, the main cluster, the zona incerta cluster and the optic tract cluster, although variations do exist (Kruger et al., 2010; Bhagwandin et al., 2011a,b; Gravett et al., 2011; Dell et al., 2012, 2013; Calvey et al., 2013; Maseko et al., 2013; Patzke et al., 2014). One of the interesting variations found was the existence of a medially located parvocellular cluster of orexinergic neurons in the giraffe and harbour porpoise (Dell et al., 2012), which has since been reported in the African elephant (Maseko et al., 2013). Thus, the Cetartiodactyla as a group appear to have an additional orexinergic

nucleus normally not observed in other mammals. Despite this and other variations (Kruger et al., 2010), the general organization of the nuclear subdivisions of this system is conserved across the mammals that have been studied to date.

A similar consistency in the arrangement of the orexinergic terminal networks was observed in the cerebral cortex of the 12 Cetartiodactyla species investigated in the current study. In all species, in both cortical areas investigated, orexinergic boutons could be classified into two size classes (large and small). Interestingly, the size of both the large and small boutons, and the proportions of small and large boutons, were very consistent across the Cetartiodactyla species studied, showing no changes associated with brain mass, neuron density, glia density, or glia:neuron ratio, despite the cetaceans studied having significantly higher glia densities, and markedly higher glia:neuron ratios, than the artiodactyls studied. In addition, it is well known that cetaceans sleep in a manner that is very different to other mammals (Lyamin et al., 2008), a physiological process that is likely, in part, to be dependent upon the orexinergic system. Thus, it would appear that if the orexinergic system is involved in producing cetacean-type sleep, it must occur at a level of organization that does not involve the addition or loss of hypothalamic orexinergic nuclei or changes in the appearance, size and proportions of the orexinergic boutons within the cerebral cortex when compared to the closely related artiodactyls. The fact that this system exhibits a very conserved morphology indicates that changes in quantity, rather than quality, may lie at the root of observable physiological differences associated with sleep between artiodactyl and cetacean species.

4.2. Differences between artiodactyl and cetacean orexinergic boutons

Given the extensive similarity in the morphology of the boutons forming the orexinergic terminal networks in the cerebral cortex of the Cetartiodactyla, the finding that, even when brain mass, neuronal density, glia density and glia:neuron ratio are taken into account, cetaceans have a significantly lower density of orexinergic boutons compared to artiodactyls forms one of the central findings of the current study. Given our earlier finding that the harbour porpoise has significantly more orexinergic neurons in the hypothalamus than the giraffe (Dell et al., 2012), this indicates that despite the lower number of cells, the orexinergic axons of the giraffe provide a denser innervation of the cerebral cortex than those of the harbour porpoise. This arrangement is likely to be found across the Cetartiodactyla, with artiodactyls having a denser orexinergic innervation of the cerebral cortex than the cetaceans, as observed in the species analyzed in the current study; however, counts of the numbers of orexinergic neurons in the hypothalami of the species studied will be needed to confirm this generalization. Despite this, it would seem appropriate, at the current time, to conclude that the orexinergic innervation of the cerebral cortex is lower in cetaceans generally than in artiodactyls – a distinct quantitative difference.

This likely quantitative difference in orexinergic bouton density might be a result of the horizontal expansion of the cetacean cerebral cortex in comparison to other mammals. Cetaceans are known to have a very large cortical surface area (Ridgway and Brownson, 1984) and a highly gyrencephalic cerebral cortex (Manger et al., 2012) in comparison to other mammals. Despite this, we found that when we compared bouton density to brain

mass, neuronal density, glia density and glia:neuron ratio, the cetaceans studied were still found to have a lower orexinergic density than the artiodactyls studied. Thus, with appropriate comparisons that should correct for potential differences in the cetacean cerebral cortex, the orexinergic innervation was still found to be lower in the cetaceans studied than that found in the artiodactyls studied.

A second observation of interest was the consistently higher density of orexinergic boutons in the anterior cingulate cortex when compared to the occipital cortex in most of the artiodactyls studied, except for the domestic pig. In the cetaceans, the bouton density was similar in both cortical regions. Thus, it would appear that in general, the anterior cingulate cortex of artiodactyls receives a stronger orexinergic innervation than the occipital cortex, but this does not occur in the cetaceans. The anterior cingulate cortex is functionally correlated with arousal, attention, behavior and cognition; hence it is likely that the orexinergic innervation of the anterior cingulate cortex would contribute to these functions (Hofle et al., 1997; Peyron et al., 1998; Yamasaki et al., 2002; Song et al., 2006; Yamada et al., 2008). Studies of the rat medial prefrontal cortex have shown that orexinergic post-synaptic excitation of pyramidal neurons leads to an arousal related to food, specifically energy balance, as the orexin receptors are sensitive to glucose and leptin (Song et al., 2006; Fadel and Frederick-Duus, 2008). Given the starch-based, herbivorous diet of artiodactyls, it is possible that artiodactyls would require more orexinergic boutons in the anterior cingulate cortex to monitor energy balance and appetitive drive. In contrast, cetaceans survive on a high protein high fat diet (Santos and Pierce, 2003) and the energy from that diet would be obtained mainly through ketosis, which would give rise to gluconeogenesis (Pichon et al., 2006). As the glucose in a cetacean diet is obtained from an indirect pathway, the demand for glucose to be monitored by orexinergic boutons in the anterior cingulate cortex may be of less important. One could propose that energy balance in response to glucose is the driving factor for the variations observed in the orexinergic system and thus for arousal, and this is in line with the speculations made by Dell et al. (2012). This speculation is supported by the reduced density of orexinergic boutons in the anterior cingulate cortex of the domestic pig, which is primarily an omnivore and thus would consume a mixed diet of starch, protein and fats. Given that arousal and food consumption are inextricably linked in mammals (finding and ingesting food while asleep is unlikely to occur), it would appear that the cetaceans, while experiencing the evolution of an unusual form of mammalian sleep (Lyamin et al., 2008), may have also experienced changes associated with the cortical loci regulating energy balance and appetitive drive.

4.3. Orexinergic bouton and glial cell density interaction in the cetacean cerebral cortex

The principal components analysis undertaken in the current study indicates that orexinergic bouton density in the cerebral cortex appears to be primarily correlated with glial cell density, with an inverse correlation existing between orexinergic bouton density and glial density. The cetaceans studied were found to have lower orexinergic bouton densities and higher glial densities than the artiodactyls studied. While glial cells are associated with a broad range of functions, one vital role that astrocytes play is lactate production (Parsons and Hirasawa, 2010). Speculatively, an increased number of glial cells in the cetacean brain, as seen herein when compared to artiodactyls, may result in an increased production of

lactate. This extracellular lactate may be related to maintained arousal and attention during unihemispheric sleep (Ridgway et al., 2006, 2009; Branstetter et al., 2012), as extracellular lactate concentrations are higher during periods of wake (Pellerin and Magistretti, 1994). Furthermore lactate reduces extracellular pH levels and this is vital for arousal and attention, as orexinergic neurons are excited by a low pH (Williams et al., 2007; Parsons and Hirasawa, 2010). Perhaps orexinergic neurons and their axonal projections do not only contribute to arousal and appetitive drive, but also to the interaction that exists between the orexinergic neurons and their projections, glial cells, and the biochemical correlates of nutrition. It is possible that further research testing this idea might lead to a clearer understanding of the function of the orexinergic system in both arousal and appetitive drive and the variation reported herein for two species of cetaceans.

4.4. Communication channels and the large and small orexinergic boutons

While it has been demonstrated that orexin induces a post-synaptic excitatory effect on cortical neurons (Song et al., 2006; Yan et al., 2012), the specific channel of communication that enacts this effect is presently unknown – do the axonal terminations of the orexinergic axons form specific synaptic connections, or do they act through volume transmission (Fuxe et al., 2010)? The current study does not directly answer this question, but does indicate two specific potential answers. Our observations in this study indicate that there are both larger and smaller orexinergic boutons present on the arborizing orexinergic axonal terminals. This means that it is possible that synaptic chemical transmission, volume transmission, or both may be occurring in the cerebral cortex. A recent study showed that orexin could be released through both chemical synaptic transmission and through volume transmission (Del Cid-Pellitero and Garzón, 2011). Orexin released from non-synaptic orexinergic axon varicosities in the dorsal raphe diffused through the extracellular space and activated distant high affinity receptors, providing a longer sustained activation than orexin released through chemical synaptic transmission (Del Cid-Pellitero and Garzón, 2011). Thus, it appears that the excitatory action of orexin in the cerebral cortex might be initiated through two different communication channels. This clearly dovetails nicely with the current observations of two different orexinergic bouton types within the cerebral cortex of the animals studied herein. Understanding these two potential channels of communication and the effect they may exert on target neurons or other cells of the central nervous system, using such methods as transmitter receptor mismatch at an ultrastructural level as suggested Del Cid-Pellitero and Garzón (2011), may provide important insights into the function of orexin in the cerebral cortex and the effect that variations in bouton densities and sizes may play in different mammalian species.

Acknowledgments

This work was mainly supported by funding from the South African National Research Foundation (P.R.M., N.C.B.) and by a fellowship within the Postdoctoral-Program of the German Academic Exchange Service, DAAD (N.P.). The work was also supported by an IOER R&G Grant from Des Moines University (#12-13-03) (M.A.S.), Reykjavik University 2010 Development Fund (K.Æ.K.), the Deanship of Scientific Research at the King Saud University through the research group project number RGP_020 (A.N.A., O.B.M.), and NIH grant DA 2R01MH064109 and the Department of Veterans Affairs (J.M.S).

References

Alexandre C, Andermann ML, Scammell TE, 2013. Control of arousal by the orexin neurons. Curr. Opin. Neurobiol 23, 752–759. [PubMed: 23683477]

Badlangana NL, Adams JW, Manger PR, 2009. The giraffe (*Giraffa camelopardalis*) cervical vertebral column: a heuristic example in understanding evolutionary processes. Zool. J. Linn. Soc 155, 736–757.

Bayer L, Serafin M, Eggermann E, Saint-Mleux B, Machard D, Jones BE, Muhlethaler M, 2004. Exclusive postsynaptic action of hypocretin-orexin on sublayer 6b cortical neurons. J. Neurosci 24, 6760–6764. [PubMed: 15282280]

Bell FR, Itabisashi T, 1973. The electroencephalogram of sheep and goats with special reference to rumination. Physiol. Behav 11, 503–514. [PubMed: 4355157]

Bhagwandin A, Fuxe K, Bennett NC, Manger PR, 2011a. Distribution of orexinergic neurons and their terminal networks in the brains of two species of African mole rats. J. Chem. Neuroanat 41, 32–42. [PubMed: 21093582]

Bhagwandin A, Gravett N, Hemingway J, Oosthuizen MK, Bennett NC, Siegel JM, Manger PR, 2011b. Orexinergic neuron numbers in three species of African mole rats with rhythmic and arrhythmic chronotypes. Neuroscience 199, 153–165. [PubMed: 22056958]

Blouin AM, Fried I, Wilson CL, Staba RJ, Behnke EJ, Lam HA, Maidment NT, Karlsson KÆ, Lapierre JL, Siegel JM, 2013. Human hypocretin and melanin-concentrating hormone levels are linked to emotion and social interaction. Nat. Commun 4, 1547. [PubMed: 23462990]

Branstetter BK, Finneran JJ, Flethcer EA, Weisman BC, Ridgway SH, 2012. Dolphins can maintain vigilant behavior through echolocation for 15 days with interruption or cognitive impairment. PLoS ONE 7, e47478. [PubMed: 23082170]

Calvey T, Patzke N, Kaswera C, Gilissen E, Bennett NC, Manger PR, 2013. Nuclear organization of some immunohistochemically identifiable neural systems in three Afrotherian species – *Potomogale velox*, *Amblysomus hottentotus* and *Petrodromus tetradactylus*. J. Chem. Neuroanat 50–51, 48–65.

Datta S, MacLean RR, 2007. Neurobiological mechanisms for the regulation of mammalian sleep–wake behavior: reinterpretation of historical evidence and inclusion of contemporary cellular and molecular evidence. Neurosci. Biobehav. Rev 31, 775–824. [PubMed: 17445891]

Del Cid-Pellitero E, Garzón M, 2011. Hypocretin1/orexin-A immunoreactive axons form few synaptic contacts on rat ventral tegmental area neurons that project to the medial prefrontal cortex. BMC Neurosci. 7 (15), 105.

Dell LA, Patzke N, Bhagwandin A, Bux F, Fuxe K, Barber G, Siegel JM, Manger PR, 2012. Organization and number of orexinergic neurons in the hypothalamus of two species of Cetartiodactyla: a comparison of giraffe (*Giraffa camelopardalis*) and harbour porpoise (*Phocoena phocoena*). J. Chem. Neuroanat 44, 98–109. [PubMed: 22683547]

Dell LA, Kruger JL, Pettigrew JD, Manger PR, 2013. Cellular location and major terminal networks of the orexinergic system in the brain of two megachiropterans. J. Chem. Neuroanat 53, 64–71. [PubMed: 24041616]

Edwards CM, Abusnana S, Sunter D, Murphy KG, Ghatei MA, Bloom SR, 1999. The effect of the orexins on food intake: comparison with neuropeptide Y, melanin-concentrating hormone and galanin. J. Endocrinol 160, R7–R12. [PubMed: 10077743]

Ettrup KS, Srensen JS, Bjarkam CR, 2010. The anatomy of the Göttingen minipig hypothalamus. J. Chem. Neuroanat 39, 151–165. [PubMed: 20043984]

Fadel J, Frederick-Duus D, 2008. Orexin/hypocretin modulation of the basal forebrain cholinergic system: insights from in vivo microdialysis studies. Pharmacol. Biochem. Behav 90, 156–162. [PubMed: 18281084]

Fuxe K, Dahlstrom AB, Jonsson G, Marcellino D, Guescini M, Dam M, Manger P, Agnati L, 2010. The discovery of central monoamine neurons gave volume transmission to the wired brain. Prog. Neurobiol 90, 82–100. [PubMed: 19853007]

Gravett N, Bhagwandin A, Fuxe K, Manger PR, 2011. Distribution of orexin-A immunoreactive neurons and their terminal networks in the brain of the rock hyrax, *Procavia capensis*. J. Chem. Neuroanat 41, 86–96. [PubMed: 21126575]

Gundersen HJ, Bagger P, Bendtsen TF, Evans SM, Korbo L, Marcussen N, Moller A, Nielsen K, Nyengaard JR, Pakkenberg B, Sorensen FB, Vesterby A, West MJ, 1988. The new stereological tools: disector, fractionator, nucleator and point sampled intercepts and their use in pathological research and diagnosis. APMIS 96, 857–881. [PubMed: 3056461]

Gundersen HJ, Jensen EB, 1987. The efficiency of systematic sampling in stereology and its prediction. J. Microsc 147, 229–263. [PubMed: 3430576]

Hofle N, Paus T, Reutens D, Fiset P, Gotman J, Evans AC, Jones BE, 1997. Regional cerebral blood flow changes as a function of delta and spindle activity during slow wave sleep in humans. J. Neurosci 17, 4800–4808. [PubMed: 9169538]

Horvath TL, Peyron C, Diano S, Ivanov A, Aston-Jones G, Kilduff TS, van den Pol AN, 1999. Hypocretin (orexin) activation and synaptic innervation of the locus coeruleus noradrenergic system. J. Comp. Neurol 415, 145–159. [PubMed: 10545156]

Iqbal J, Pompolo S, Sakurai T, Clarke IJ, 2001. Evidence that orexin-containing neurons provide direct input to gonadotrophin-releasing hormone neurones in the ovine hypothalamus. J. Neuroendocrinol 13, 1033–1041. [PubMed: 11722699]

Jessen C, 1998. Brain cooling: an economy mode of temperature regulation in artiodactyls. News Physiol. Sci 13, 281–286. [PubMed: 11390804]

Jessen C, 2001. Selective brain cooling in mammals and bird. Jpn. J. Physiol 51, 291–301. [PubMed: 11492953]

Johnson JI, 1990. Chapter 15. Comparative development of somatic sensory cortex. In: Jones EG, Peters A (Eds.), Cerebral Cortex Volume 8B. Comparative Structure and Evolution of Cerebral Cortex, Part II Plenum Press, New York, pp. 335–449.

Kruger J-L, Dell L-A, Pettigrew JD, Manger PR, 2010. Cellular location and major terminal networks of the orexinergic system in the brains of five microchiropteran species. J. Chem. Neuroanat 40, 256–262. [PubMed: 20654711]

Kuhnen G, 1997. Selective brain cooling reduces respiratory water loss during heat stress. Comp. Biochem. Physiol. A: Physiol 118, 891–895. [PubMed: 9406453]

Lyamin OI, Manger PR, Ridgway SH, Muhametov LM, Siegel JM, 2008. Cetacean sleep: an unusual form of mammalian sleep. Neurosci. Biobehav. Rev 32, 1451–1484. [PubMed: 18602158]

Manger PR, 2006. An examination of cetacean brain structure with a novel hypothesis correlating thermogenesis to the evolution of a big brain. Biol. Rev. Camb. Philos. Soc 81, 293–338. [PubMed: 16573845]

Manger PR, Pillay P, Maseko BC, Bhagwandin A, Gravett N, Moon DJ, Jillani NE, Hemingway J, 2009. Acquisition of the brain of the African elephant (*Loxodonta africana*): perfusion-fixation and dissection. J. Neurosci. Methods 179, 16–21. [PubMed: 19168095]

Manger PR, Prowse M, Haagensen M, Hemingway J, 2012. Quantitative analysis of neocortical gyrencephaly in African elephants (*Loxodonta africana*) and six species of cetaceans: comparison with other mammals. J. Comp. Neurol 520, 2430–2439. [PubMed: 22237903]

Maseko BC, Patzke N, Fuxe K, Manger PR, 2013. Architectural organization of the African elephant diencephalon and brainstem. Brain Behav. Evol 82, 83–128. [PubMed: 24021932]

McGregor R, Wu M-F, Barber G, Ramanathan L, Siegel JM, 2011. Highly specific role of hypocretin (orexin) neurons: differential activation as a function of diurnal phase, operant reinforcement vs. operant avoidance and light level. J. Neurosci 31, 15455–15467. [PubMed: 22031892]

Mileykovskiy BY, Kiyashchenko LI, Siegel JM, 2005. Behavioral correlates of activity in identified hypocretin/orexin neurons. Neuron 46, 787–798. [PubMed: 15924864]

Mintz EM, van den Pol AN, Casano AA, Albers HE, 2001. Distribution of hypocretin (orexin) immunoreactivity in the central nervous system of Syrian hamsters (*Mesocricetus auratus*). J. Chem. Neuroanat 21, 225–238. [PubMed: 11382534]

Mitchell D, Maloney SK, Jessen C, Laburn HP, Kamerman PR, Mitchell G, Fuller A, 2002. Adaptive heterothermy and selective brain cooling in arid-zone mammals. Comp. Biochem. Physiol. B: Biochem. Mol. Biol 131, 571–585. [PubMed: 11923074]

Moore RY, Abrahamson EA, van den Pol A, 2001. The hypocretin neuron system: an arousal system in the human brain. Arch. Ital. Biol 139, 195–206. [PubMed: 11330201]

Nambu T, Sakurai T, Mizuhami K, Hosoya Y, Yanagisawa M, Goto K, 1999. Distribution of orexin neurons in the adult rat brain. Brain Res. 827, 243–260. [PubMed: 10320718]

Nixon JP, Smale L, 2007. A comparative analysis of the distribution of immunoreactive orexin A and B in the brain of nocturnal and diurnal rodents. Behav. Brain Funct 3, 28. [PubMed: 17567902]

Parsons MP, Hirasawa M, 2010. ATP-sensitive potassium channel-mediated lactate effect on orexin neurons: implications for brain energetics during arousal. J. Neurosci 30, 8061–8070. [PubMed: 20554857]

Patzke N, Bertelsen MF, Fuxe K, Manger PR, 2014. Nuclear organization of cholinergic, catecholaminergic, serotonergic and orexinergic systems in the brain of the Tasmanian devil (*Sarcophilus harrisii*). J. Chem. Neuroanat 61–62, 94–106.

Pellerin L, Magistretti PJ, 1994. Glutamate uptake into astrocytes stimulates aerobic glycolysis: a mechanism coupling neuronal activity to glucose utilization. Proc. Natl. Acad. Sci. U. S. A 91, 10625–10629. [PubMed: 7938003]

Peyron C, Tighe DK, van den Pol AN, de Lecea L, Heller HC, Sutcliffe JG, Kilduff TS, 1998. Neurons containing hypocretin (orexin) project to multiple neuronal systems. J. Neurosci 18, 9996–10015. [PubMed: 9822755]

Pichon L, Huneau J, Fromentin G, Tomé D, 2006. A high-protein, high-fat, carbohydrate-free diet reduces energy intake, hepatic lipogenesis, and adiposity in rats. J. Nutr 136, 1256–1260. [PubMed: 16614413]

Price SA, Bininda-Emonds OR, Gittleman JL, 2005. A complete phylogeny of the whales, dolphins and even-toed hoofed mammals (*Cetartiodactyla*). Biol. Rev. Camb. Philos. Soc 80, 445–473. [PubMed: 16094808]

Ridgway SH, Brownson RH, 1984. Relative brain sizes and cortical surface areas in odontocetes. ACTA Zool. Fenn 172, 149–152.

Ridgway S, Carder D, Finneran J, Keogh M, Kamolnick T, Todd M, Goldblatt A, 2006. Dolphin continuous auditory vigilance for five days. J. Exp. Biol 209, 3621–3628. [PubMed: 16943502]

Ridgway S, Keogh M, Carder D, Finneran J, Kamolnick T, Todd M, Goldblatt A, 2009. Dolphins maintain cognitive performance during 72 to 120 hours of continuous auditory vigilance. J. Exp. Biol 212, 1519–1527. [PubMed: 19411545]

Sakurai T, Amemiya A, Ishii M, Matsuzaki I, Chemelli RM, Tanaka H, Williams SC, Richardson JA, Kozlowski GP, Wilson S, Arch JRS, Buckingham RE, Haynes AC, Carr SA, Annan RS, McNulty DE, Liu WS, Terrett JA, Elshourbagy NA, Bergsma DJ, Yanagisawa M, 1998. Orexins and orexin receptors: a family of hypothalamic neuropeptides and G protein-coupled receptors that regulate feeding behavior. Cell 92, 573–585. [PubMed: 9491897]

Santos MB, Pierce GJ, 2003. The diet of harbour porpoise (*Phocoena phocoena*) in the northeast Atlantic. Oceanogr. Mar. Biol. Ann. Rev 41, 355–390.

Schenker NM, Hopkins WD, Spocter MA, Garrison AR, Stimpson CD, Erwin JM, Hof PR, Sherwood CC, 2010. Broca's area homologue in chimpanzee (*Pan troglodytes*): probabilistic mapping, asymmetry, and comparison to humans. Cereb. Cortex 20, 730–742. [PubMed: 19620620]

Schmitz C, Hof PR, 2000. Recommendations for straightforward and rigorous methods of counting neurons based on a computer simulation approach. J. Chem. Neuroanat 20, 93–114. [PubMed: 11074347]

Song C, Chen X, Xia J, Yu Z, Hu Z, 2006. Modulatory effects of hypocretin-1/orexin-A with glutamate and γ-aminobutyric acid on freshly isolated pyramidal neurons from the rat prefrontal cortex. Neurosci. Lett 399, 101–105. [PubMed: 16495001]

Spinazzi R, Andries PG, Rossi GP, Nussdorfer GG, 2006. Orexins in the regulation of the hypothalamic-pituitary-adrenal axis. Pharmacol. Rev 58, 46–57. [PubMed: 16507882]

Thannickal TC, Lai YY, Siegel JM, 2007. Hypocretin (orexin) cell loss in Parkinson's disease. Brain 130, 1586–1595. [PubMed: 17491094]

Tobler I, Schwierin B, 1996. Behavioural sleep in the giraffe (*Giraffa camelopardalis*) in a zoological garden. J. Sleep Res 5, 21–32. [PubMed: 8795798]

van den Pol AN, 1999. Hypothalamic hypocretin (orexin): robust innervation of the spinal cord. J. Neurosci 19, 3171–3182. [PubMed: 10191330]

Wagner D, Salin-Pascual R, Greco MA, Shiromani PJ, 2000. Distribution of hypocretin-containing neurons in the lateral hypothalamus and c-fos-immunoreactive neurons in the VLPO. Sleep Res. Online 3, 35–42. [PubMed: 11382898]

West MJ, Slomianka L, Gundersen HJ, 1991. Unbiased stereological estimation of the total number of neurons in the subdivisions of the rat hippocampus using the optical fractionator. Anat. Rec 231, 482–497. [PubMed: 1793176]

Williams RH, Jensen LT, Verkhratsky A, Fugger L, Burdakov D, 2007. Control of hypothalamic orexin neurons by acid and CO_2. Proc. Natl. Acad. Sci. U. S. A 104, 10685–10690. [PubMed: 17563364]

Yamada N, Katsuura G, Tatsuno I, Asaki T, Kawahara S, Ebihara K, Nakao K, 2008. Orexin decreases mRNA expressions of NMDA and AMPA receptor subunits in rat primary neuron circuits. Peptides 29, 1582–1587. [PubMed: 18573570]

Yamasaki H, LaBar KS, McCarthy G, 2002. Dissociable prefrontal brain systems for attention and emotion. Proc. Natl. Acad. Sci. U. S. A 99, 11447–11451. [PubMed: 12177452]

Yan J, He C, Xia J, Zhang D, Hu Z, 2012. Orexin-A excites pyramidal neurons in layer 2/3 of the rat prefrontal cortex. Neurosci. Lett 520, 92–97. [PubMed: 22617634]

Yoshida K, McCormack S, España RA, Crocker A, Scammell TE, 2006. Afferents to the orexin neurons of the rat brain. J. Comp. Neurol 494, 845–861. [PubMed: 16374809]

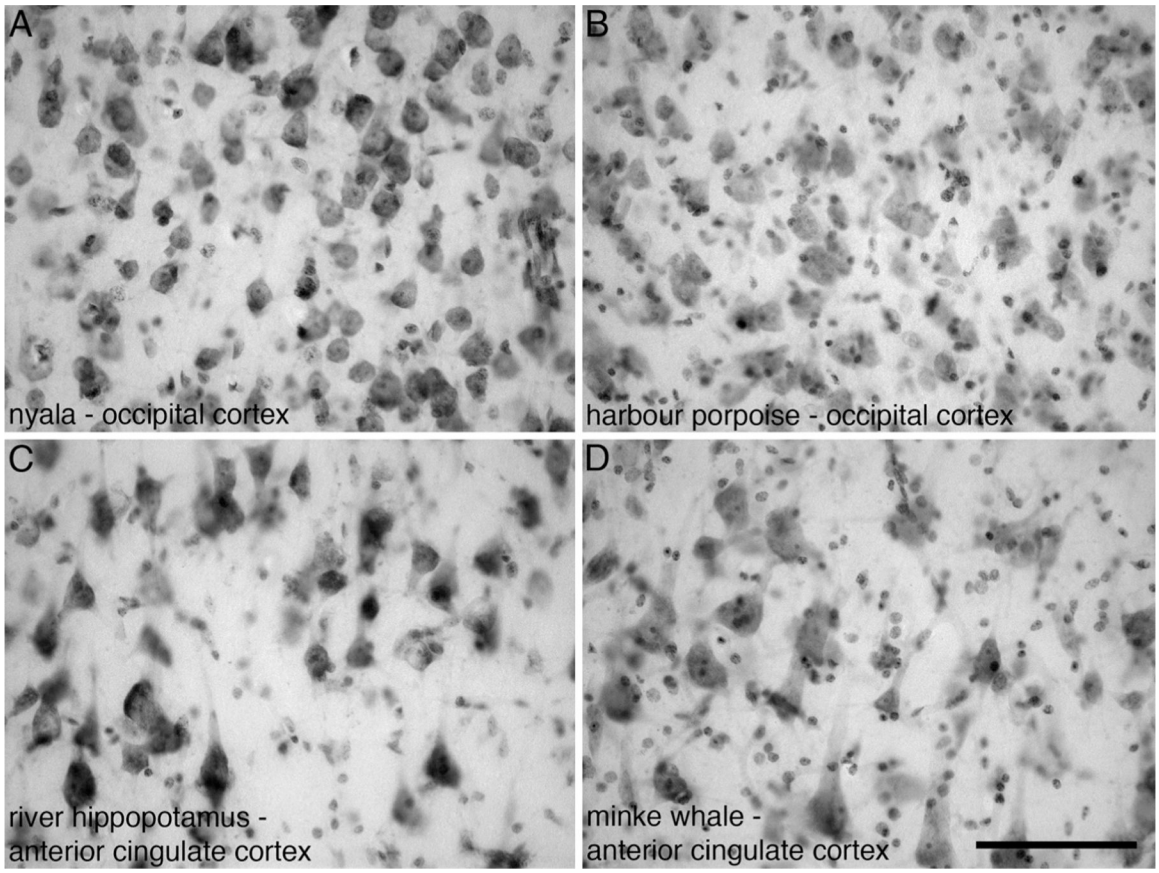

Fig. 1.

Photomicrographs of Nissl stained sections from layer III in the occipital cortex (A, B) and anterior cingulate cortex (C, D) of four different species of Cetartiodactyla examined in the present study showing the neuronal and glia profiles used for stereological analysis. (A) Nyala (*Tragelaphus angasii*). (B) Harbour porpoise (*Phocoena phocoena*). (C) River hippopotamus (*Hippopotamus amphibius*). (D) Minke whale (*Balaenoptera acutorostratus*). Scale bar in D = 100 μm and applies to all.

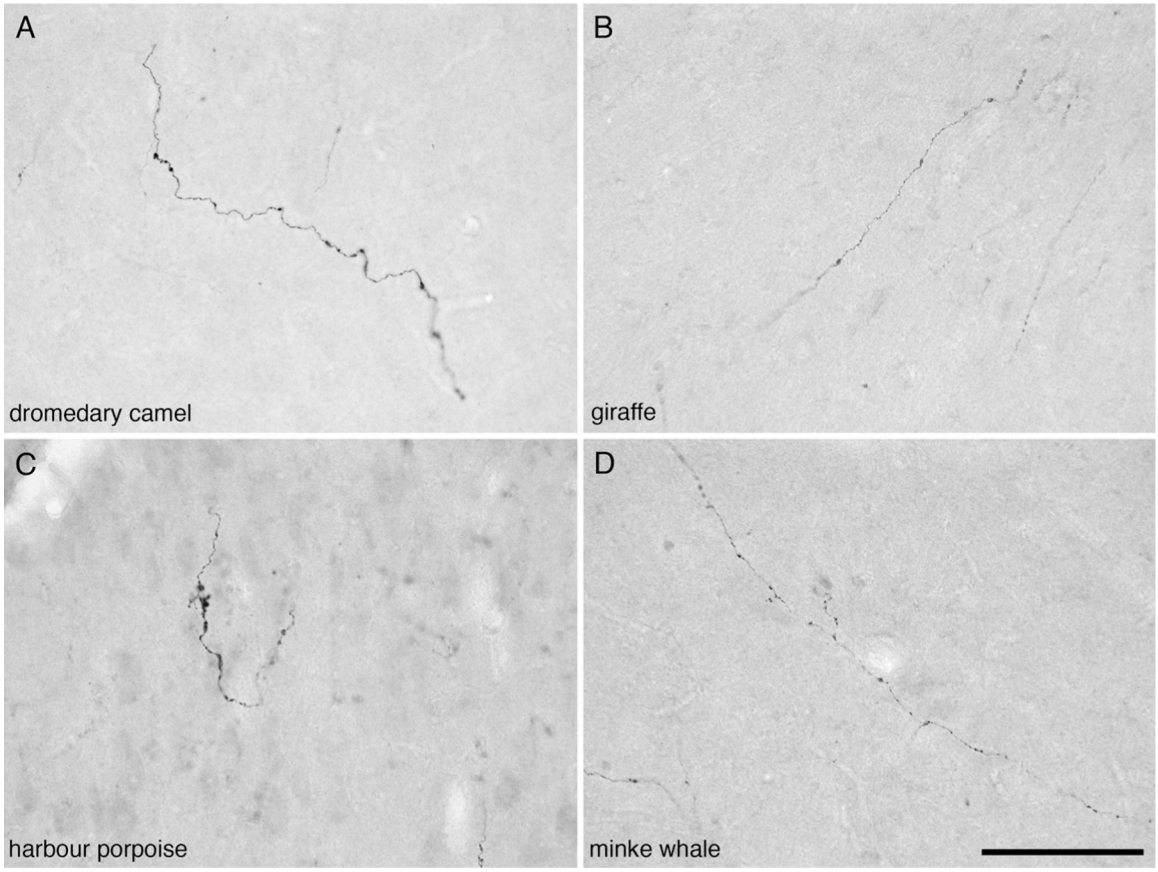

Fig. 2.

Photomicrographs of orexinergic axons, showing boutons, in layer III of the anterior cingulate cortex of four different species of Cetartiodactyla examined in the present study. (A) Dromedary camel (*Camelus dromedarius*). (B) Giraffe (*Giraffa camelopardalis*). (C) Harbour porpoise (*Phocoena phocoena*). (D) Minke whale (*Balaenoptera acutorostratus*). Scale bar in D = 100 μm and applies to all.

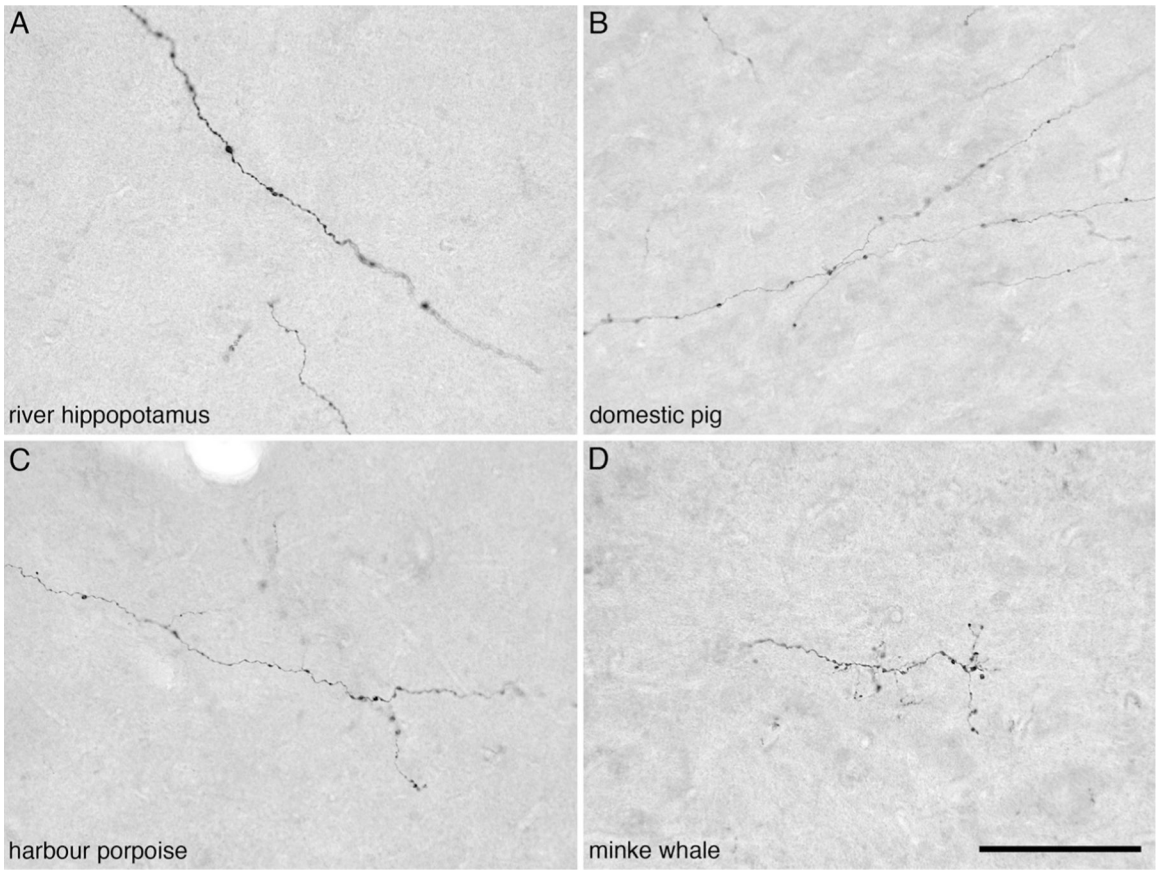

Fig. 3.

Photomicrographs of orexinergic axons, showing boutons, in layer III of the occipital cortex of four different species of Cetartiodactyla examined in the present study. (A) River hippopotamus (*Hippopotamus amphibius*). (B) Domestic pig (*Sus scrofa*). (C) Harbour porpoise (*Phocoena phocoena*). (D) Minke whale (*Balaenoptera acutorostratus*). Scale bar in D = 100 μm and applies to all.

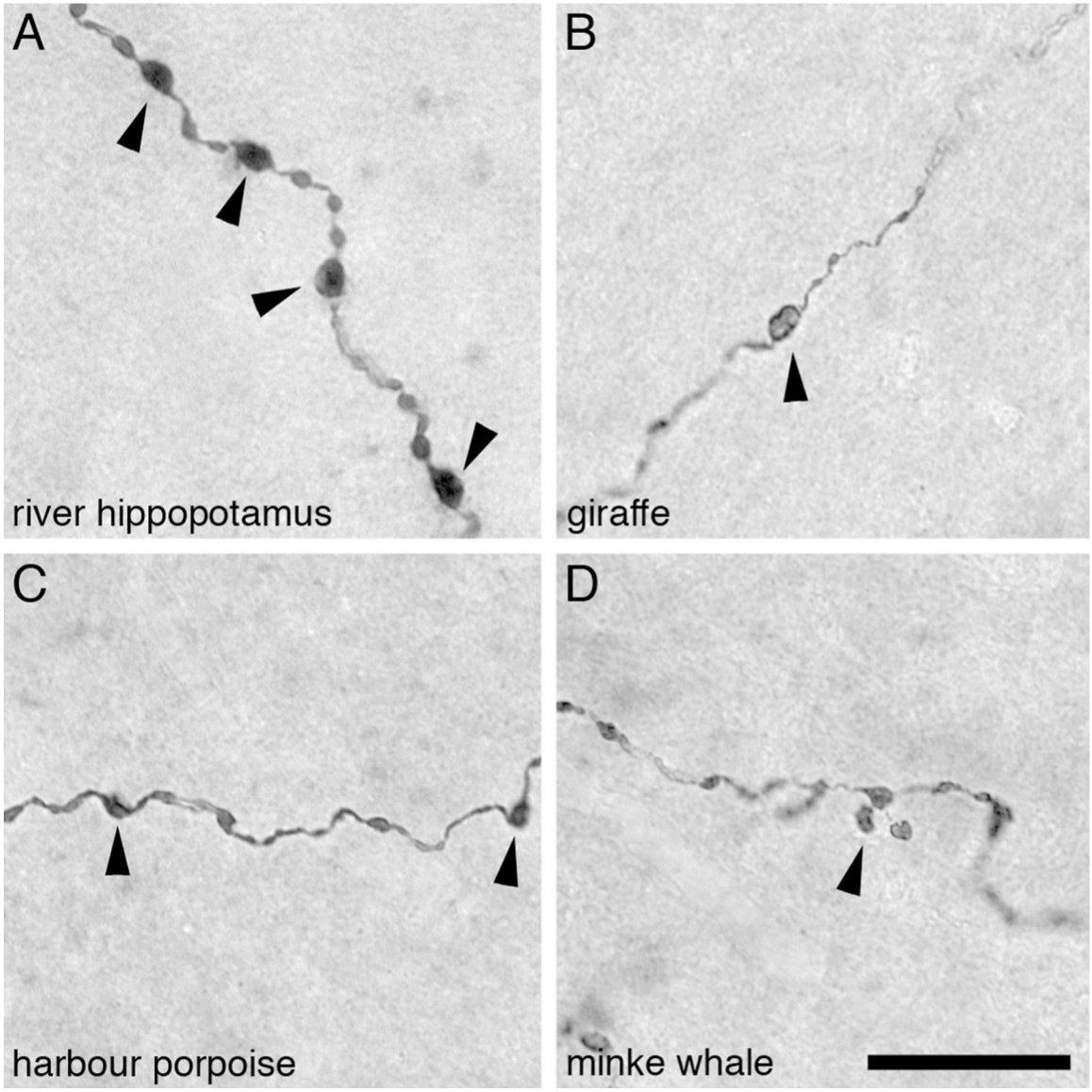

Fig. 4.

High power photomicrographs of orexinergic axons, showing the appearance of the large and small orexinergic boutons, in layer III of the cerebral cortex of four different species of Cetartiodactyla examined in the present study. (A) River hippopotamus (*Hippopotamus amphibius*). (B) Giraffe (*Giraffa camelopardalis*). (C) Harbour porpoise (*Phocoena phocoena*). (D) Minke whale (*Balaenoptera acutorostratus*). In all images the arrowheads indicate the boutons considered to be large boutons, while the small boutons have been left unmarked. Scale bar in D = 20 μm and applies to all.

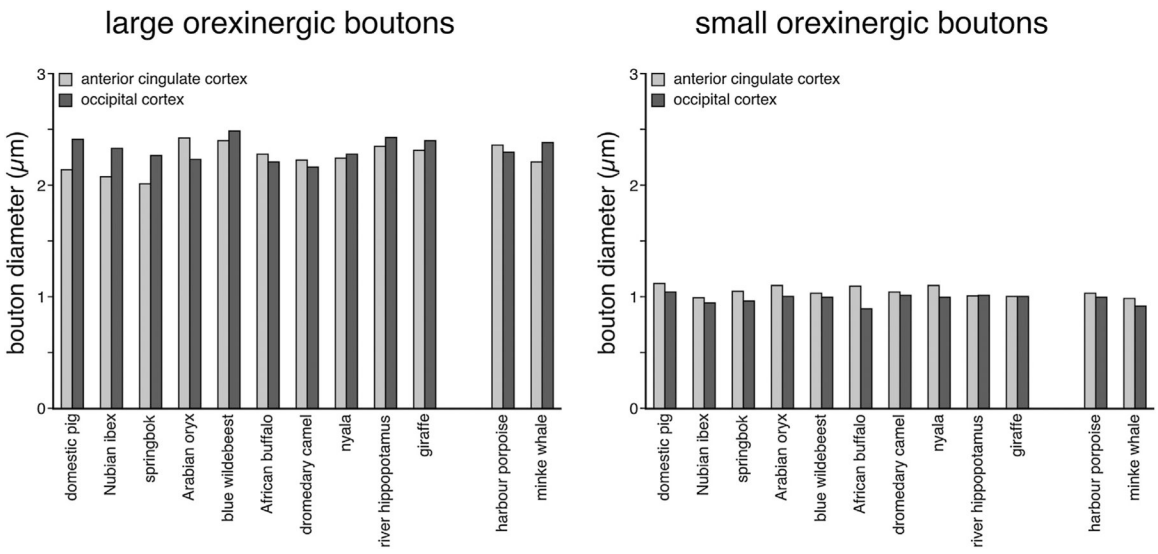

Fig. 5.

Bar graphs showing the average diameter of the large and small orexinergic boutons in the anterior cingulate and occipital cortex of all species studied. Note the similarity in average size of both large and small orexinergic boutons across both cortical areas and all species examined.

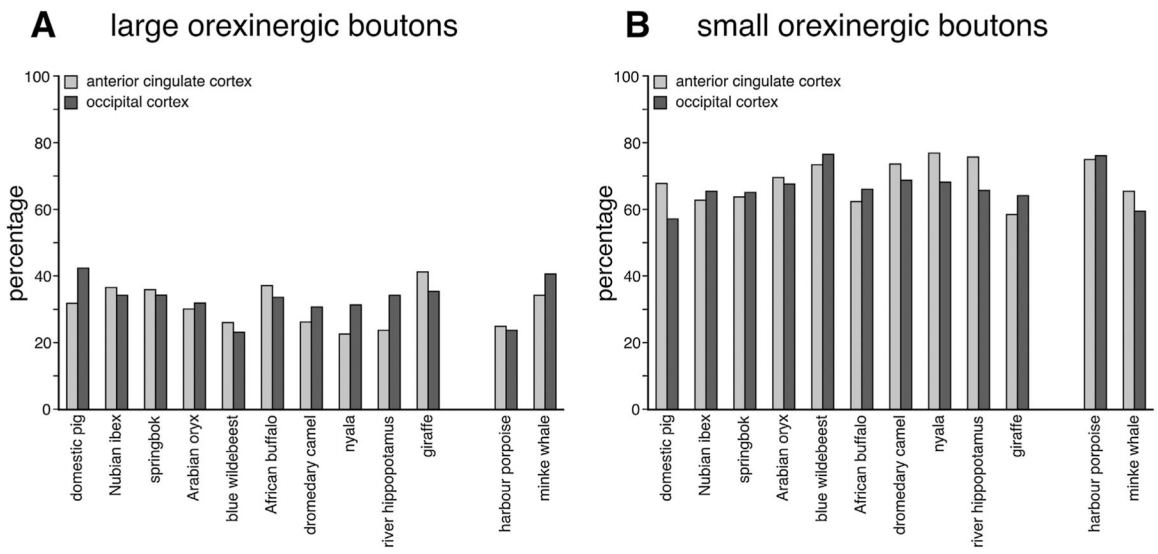

Fig. 6.

Bar graphs showing the percentage of large (A) and small (B) orexinergic boutons in the anterior cingulate and occipital cortex of all species studied. Note the far greater number of smaller orexinergic boutons in all species, and the similar percentages of both large and small boutons across all species.

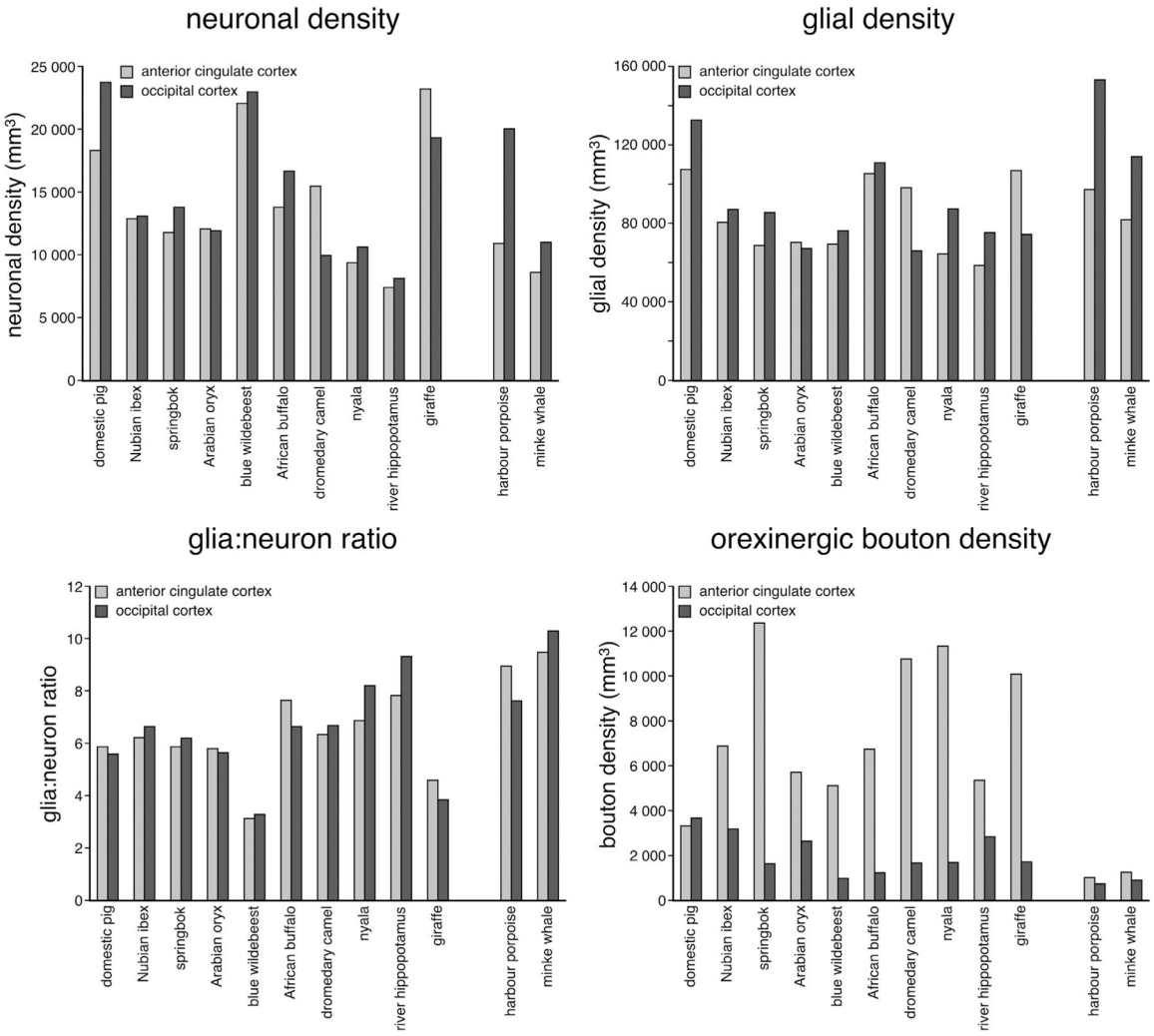

Fig. 7.

Bar graphs showing the neuronal density, glial density, and glia:neuron ratio and orexinergic bouton density in the anterior cingulate and occipital cortex across all species studied. Note the slightly higher glial density and higher glia:neuron ratios in the cetacean brains compared to the artiodactyls studied. In addition, the orexinergic bouton density in the cetacean cerebral cortex is substantially lower than that seen in artiodactyl cerebral cortex, especially so for anterior cingulate cortex.

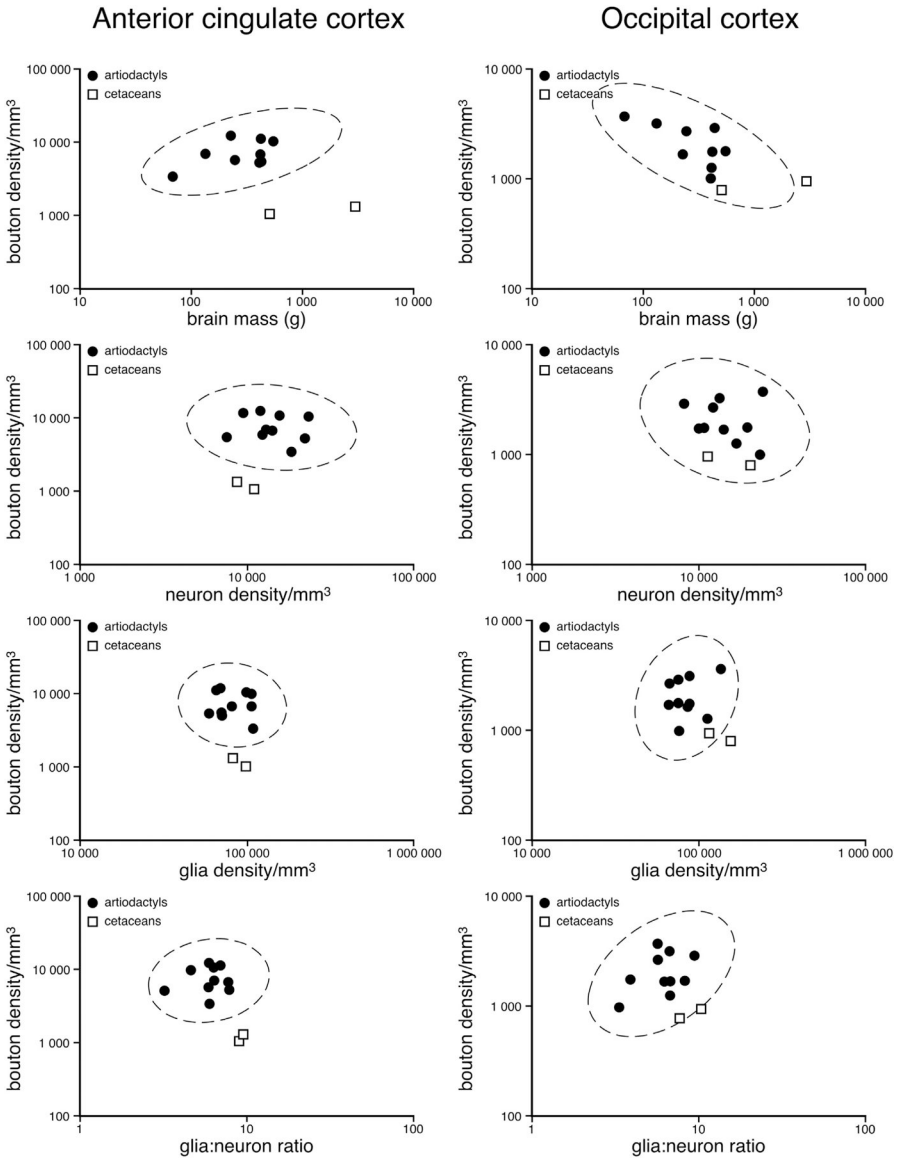

Fig. 8.

Graph depicting the statistical comparison of orexinergic bouton density in the cerebral cortex against brain mass, neuron density, glia density and glia:neuron ratios. The 95% ellipses are based on the artiodactyl data and demonstrate that for all variables compared, the cetaceans have significantly lower orexinergic bouton densities in anterior cingulate cortex than artiodactyls. In the occipital cortex, while not always statistically significant, the orexinergic bouton density of the cetaceans is often lower and always on the lower end of the range of the bouton densities when compared to artiodactyls.

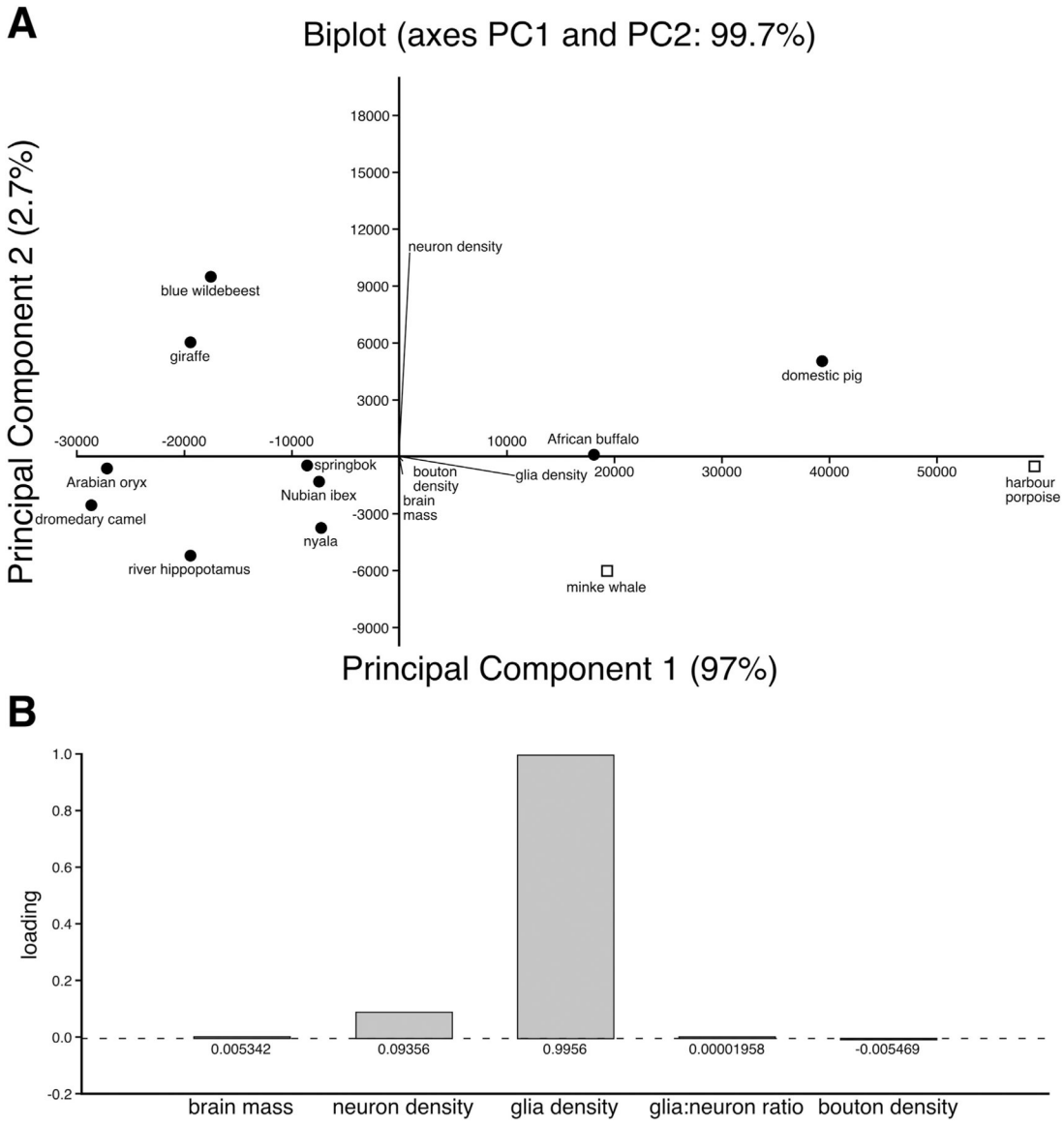

Fig. 9.

(A) Principal component analysis biplot showing the individual scatter and the variables that contributed towards differentiating the species. Principal component 1 explained 97% of the total variance while principle component 2 explained 2.7% of the total variance. The length and direction of the biplot lines determine the strength and the contribution of each of the variables to the respective principal components. For example glia density has a strong and positive influence on PC1, but a negative and weak influence on PC2. Neuron density has a positive and strong influence on PC2, but a weakly positive potentially negligible influence on PC2. Bouton density and brain mass only present with small negative associations with PC2. (B) The accompanying Factor Loadings plot showing the individual loading of the five variables on Principal component 1. Note that glial density was the most useful variable in describing the variance in Principal component 1 (i.e., factor loading ≥ 0.70).

Table 1

Stereological parameters cortex cortical neuron and glial counts. AC, anterior cingulate cortex; OC, occipital cortex.

Common name	Species name	Counting frame size (μm)	Sampling grid size (μm)	Cut thickness (μm)		Average mounted thickness (μm)		Vertical guard zones (top and bottom, percentage)	Section interval	Number of sampling sites		Average CE (Gundersen, *M* = 0)				Average CE (Gundersen, *M* = 1)			
				AC	OC	AC	OC			AC	OC	AC		OC		AC		OC	
												Neurons	Glia	Neurons	Glia	Neurons	Glia	Neurons	Glia
Domestic pig	*Sus scrofa*	80 × 80	1050 × 1050	50	50	11.8	11.7	0.01	2	112	43	0.08	0.06	0.14	0.15	0.07	0.03	0.10	0.05
Nubian ibex	*Capra nubiana*	80 × 80	1050 × 1050	50	50	10.1	9.3	0.01	2	116	56	0.14	0.04	0.14	0.11	0.08	0.04	0.10	0.05
Springbok	*Antidorcas marsupialis*	80 × 80	1050 × 1050	50	50	7.7	7.9	0.01	2	81	108	0.10	0.07	0.08	0.06	0.08	0.04	0.07	0.03
Arabian oryx	*Oryx leucoryx*	80 × 80	1050 × 1050	50	50	11.2	9.4	0.01	2	82	81	0.11	0.09	0.15	0.10	0.09	0.04	0.09	0.04
Blue wildebeest	*Connochaetes taurinus*	80 × 80	1050 × 1050	50	50	9.7	8.9	0.01	2	121	116	0.08	0.07	0.08	0.06	0.05	0.03	0.05	0.03
African buffalo	*Syncerus caffer*	80 × 80	1050 × 1050	50	50	12.1	11.5	0.01	2	130	95	0.10	0.08	0.11	0.06	0.07	0.03	0.08	0.03
Dromedary camel	*Camelus dromedarius*	80 × 80	1050 × 1050	50	50	12.4	7.8	0.01	2	57	54	0.20	0.15	0.17	0.12	0.11	0.05	0.11	0.05
Nyala	*Tragelaphus angasii*	80 × 80	1050 × 1050	50	50	8.3	9.0	0.01	2	99	82	0.11	0.07	0.09	0.08	0.08	0.04	0.09	0.03
River hippopotamus	*Hippopotamus amphibius*	80 × 80	1050 × 1050	50	50	8.3	9.0	0.01	2	135	121	0.12	0.09	0.12	0.09	0.09	0.03	0.09	0.09
Giraffe	*Giraffa camelopardalis*	80 × 80	1050 × 1050	50	50	12.1	10.4	0.01	2	86	122	0.11	0.12	0.14	0.10	0.07	0.04	0.06	0.04
Harbour porpoise	*Phocoena phocoena*	80 × 80	1050 × 1050	50	50	8.4	10.6	0.01	2	153	137	0.09	0.07	0.09	0.07	0.06	0.03	0.06	0.03
Minke whale	*Balaenoptera acutorostratus*	80 × 80	1050 × 1050	50	50	11.6	11.1	0.01	2	139	163	0.14	0.09	0.09	0.11	0.09	0.03	0.07	0.03

Table 2

Stereological parameters for orexinergic bouton counts. AC, anterior cingulate cortex; OC, occipital cortex.

Common name	Species name	Counting frame size (μm)	Sampling grid size (μm)	Rectangular width (μm)	Rectangular length (μm)	Cortical area examined ($μm^2$)	Cut thickness (μm)		Average mounted thickness (μm)		Vertical guard zones (top and bottom, μm)	Section interval	Number of sampling sites		CE (Schmitz)	
							AC	OC	AC	OC			AC	OC	AC	OC
Domestic pig	*Sus scrofa*	233.3 × 233.3	500 × 500	1500	2000	3 000 000	50	50	28.1	28.1	5	2	43	34	0.15	0.17
Nubian ibex	*Capra nubiana*	233.3 × 233.3	500 × 500	1500	1500	2 250 000	50	50	28.0	27.7	5	2	37	33	0.16	0.17
Springbok	*Antidorcas marsupialis*	233.3 × 233.3	500 × 500	1500	1500	2 250 000	50	50	30.6	29.1	5	2	33	44	0.17	0.15
Arabian oryx	*Oryx leucoryx*	233.3 × 233.3	500 × 500	1500	1500	2 250 000	50	50	28.2	28.0	5	2	37	36	0.16	0.17
Blue wildebeest	*Connochaetes taurinus*	233.3 × 233.3	500 × 500	1500	1750	2 625 000	50	50	28.7	25.4	5	2	40	45	0.16	0.15
African buffalo	*Syncerus caffer*	233.3 × 233.3	500 × 500	1500	1500	2 250 000	50	50	27.9	27.3	5	2	36	50	0.17	0.14
Dromedary camel	*Camelus dromedarius*	233.3 × 233.3	500 × 500	1500	1500	2 250 000	50	50	32.8	28.9	5	2	33	40	0.17	0.16
Nyala	*Tragelaphus angasii*	233.3 × 233.3	500 × 500	1500	1500	2 250 000	50	50	27.7	27.7	5	2	33	37	0.17	0.16
River hippopotamus	*Hippopotamus amphibius*	233.3 × 233.3	500 × 500	1500	1500	2 250 000	50	50	28.4	26.8	5	2	33	40	0.17	0.16
Giraffe	*Giraffa camelopardalis*	233.3 × 233.3	500 × 500	1500	1500	2 250 000	50	50	32.1	28.5	5	2	36	45	0.17	0.15
Harbour porpoise	*Phocoena phocoena*	233.3 × 233.3	500 × 500	1500	2000	3 000 000	50	50	29.1	28.1	5	2	60	61	0.13	0.13
Minke whale	*Balaenoptera acutorostratus*	233.3 × 233.3	500 × 500	1500	2500	3 750 000	50	50	30.8	28.4	5	2	58	94	0.13	0.10

Table 3

Results from significance testing using analysis of variance. AC, anterior cingulate cortex; OC, occipital cortex.

	df	*F*-statistic	*P* value
Dependent variable: Bouton density			
Group (Artiodactyls, Cetaceans)	1	11.112	0.003*
Brain region (AC, OC)	1	6.269	0.021*
Group * Brain region	1	5.031	0.036*
Dependent variable: Glial density			
Group (Artiodactyls, Cetaceans)	1	5.764	0.026*
Brain region (AC, OC)	1	4.462	0.047*
Group * Brain region	1	3.392	0.08*
Dependent variable: Neuron density			
Group (Artiodactyls, Cetaceans)	1	0.572	0.458
Brain region (AC, OC)	1	1.146	0.297
Group * Brain region	1	0.905	0.353
Dependent variable: Glial:neuron ratio			
Group (Artiodactyls, Cetaceans)	1	11.727	0.003*
Brain region (AC, OC)	1	0.002	0.969
Group * Brain region	1	0.060	0.809

Table 4

Summary of the data generated and used for statistical analysis in the current study. g, grams; av. dia., average diameter; % - percentage; AC, anterior cingulate cortex; OC, occipital cortex.

Common name	Species name	Brain mass (g)	Large bouton av. dia. (μm)		Small bouton av. dia. (μm)		Large bouton %		Small bouton %		Neuronal density (mm^3)		Glial density (mm^3)		Glia:neuron ratio		Orexinergic bouton density (mm^3)	
			AC	OC	AC	OC	AC	OC	AC	OC	AC	OC	AC	OC	AC	OC	AC	OC
Domestic pig	*Sus scrofa*	67	2.149	2.416	1.128	1.047	32.17	42.74	67.83	57.26	18 355	23 808	108 238	133 283	5.897	5.598	3386	3720
Nubian ibex	*Capra nubiana*	132	2.079	2.341	0.994	0.952	37.27	34.75	62.73	65.25	12 992	13 104	81 151	87 317	6.246	6.663	6910	3192
Springbok	*Antidorcas marsupialis*	224	2.031	2.277	1.049	0.961	36.36	34.86	63.64	65.14	11 808	13 887	69 440	86 121	5.881	6.202	12 351	1682
Arabian oryx	*Oryx leucoryx*	244	2.433	2.236	1.111	1.009	30.83	32.52	69.17	67.48	12 165	11 968	70 747	67 635	5.816	5.651	5699	2686
Blue wildebeest	*Connochaetes taurinus*	399	2.410	2.499	1.044	0.996	26.56	23.73	73.44	76.27	22 108	22 957	70 145	76 245	3.173	3.321	5128	996
African buffalo	*Syncerus caffer*	407	2.286	2.219	1.105	0.901	37.50	34.15	62.50	65.85	13 889	16 739	106 311	111 595	7.654	6.667	6749	1264
Dromedary camel	*Camelus dromedarius*	412	2.242	2.174	1.047	1.017	26.73	31.00	73.27	69.00	15 635	9930	99 084	66 354	6.337	6.682	10 774	1711
Nyala	*Tragelaphus angasii*	417	2.256	2.292	1.109	1.002	23.08	31.90	76.92	68.10	9432	10 718	65 040	87 719	6.896	8.184	11 335	1733
River hippopotamus	*Hippopotamus amphibius*	435	2.358	2.435	1.017	1.021	24.26	34.44	75.74	65.56	7516	8135	58 984	75 775	7.848	9.315	5392	2905
Giraffe	*Giraffa Camelopardalis*	544	2.323	2.405	1.009	1.009	41.58	35.78	58.42	64.22	23 303	19 380	107 502	74 723	4.613	3.856	10 075	1769
Harbour porpoise	*Phocoena phocoena*	503	2.371	2.309	1.036	0.999	25.22	23.94	74.78	76.06	10 938	20 129	97 623	153 415	8.925	7.622	1052	792
Minke whale	*Balaenoptera acutorostratus*	2900	2.216	2.390	0.980	0.920	34.51	40.63	65.49	59.37	8671	11 119	82 149	114 384	9.474	10.287	1317	960

J Chem Neuroanat. Author manuscript; available in PMC 2021 December 23.

Table 5

Matrix showing the results of bivariate correlation analysis for the occipital cortex (OC).

		Brain mass	OC large bouton diameter	OC small bouton diameter	OC cortical thickness	OC neuron density	OC glial density	OC glial: neuron ratio	OC bouton density
Brain mass	Correlation	1	0.179	−0.471	0.630*	−0.25	0.203	0.566	−0.454
	P value		0.577	0.122	0.028	0.434	0.526	0.055	0.138
OC large bouton diameter	Correlation	0.179	1	0.231	0.303	0.427	0.08	−0.152	0.119
	P value	0.577		0.47	0.338	0.167	0.805	0.636	0.713
OC small bouton diameter	Correlation	−0.471	0.231	1	−0.532	0.177	−0.156	−0.294	0.452
	P value	0.122	0.47		0.075	0.583	0.627	0.354	0.14
OC cortical thickness	Correlation	0.630*	0.303	−0.532	1	0.128	−0.086	−0.056	−0.571
	P value	0.028	0.338	0.075		0.692	0.79	0.864	0.052
OC neuron density	Correlation	−0.25	0.427	0.177	0.128	1	0.477	−0.668*	−0.086
	P value	0.434	0.167	0.583	0.692		0.117	0.018	0.791
OC glial density	Correlation	0.203	0.08	−0.156	−0.086	0.477	1	0.284	−0.159
	P value	0.526	0.805	0.627	0.79	0.117		0.371	0.622
OC glial:neuron ratio	Correlation	0.566	−0.152	−0.294	−0.056	−0.668*	0.284	1	−0.062
	P value	0.055	0.636	0.354	0.864	0.018	0.371		0.848
OC bouton density	Correlation	−0.454	0.119	0.452	−0.571	−0.086	−0.159	−0.062	1
	P value	0.138	0.713	0.14	0.052	0.791	0.622	0.848	

*Correlation is significant at the 0.05 level (2-tailed).

Table 6

Matrix showing the results of bivariate correlation analysis for the anterior cingulate cortex (AC).

		Brain mass	AC large bouton diameter	AC small bouton diameter	AC cortical thickness	AC neuron density	AC glial density	AC glial: neuron ratio	AC bouton density
Brain mass	Correlation	1	0.007	−0.502	0.762**	−0.307	−0.031	0.54	−0.421
	P value		0.983	0.096	0.004	0.331	0.923	0.07	0.173
AC large bouton diameter	Correlation	0.007	1	0.118	−0.029	0.131	−0.088	−0.074	−0.332
	P value	0.983		0.715	0.93	0.684	0.787	0.819	0.291
AC small bouton diameter	Correlation	−0.502	0.118	1	−0.255	0.075	0.119	−0.185	0.143
	P value	0.096	0.715		0.424	0.817	0.713	0.565	0.657
AC cortical thickness	Correlation	0.762**	−0.029	−0.255	1	−0.135	0.187	0.468	−0.760**
	P value	0.004	0.93	0.424		0.675	0.56	0.125	0.004
AC neuron density	Correlation	−0.307	0.131	0.075	−0.135	1	0.504	−0.800**	0.157
	P value	0.331	0.684	0.817	0.675		0.095	0.002	0.625
AC glial density	Correlation	−0.031	−0.088	0.119	0.187	0.504	1	0.043	−0.143
	P value	0.923	0.787	0.713	0.56	0.095		0.895	0.658
AC glial:neuron ratio	Correlation	0.54	−0.074	−0.185	0.468	−0.800**	0.043	1	−0.44
	P value	0.07	0.819	0.565	0.125	0.002	0.895		0.153
AC bouton density	Correlation	−0.421	−0.332	0.143	−0.760**	0.157	−0.143	−0.44	1
	P value	0.173	0.291	0.657	0.004	0.625	0.658	0.153	

** Correlation is significant at the 0.01 level (2-tailed).

Table 7

Matrix showing the results of bivariate correlation analysis for the anterior cingulate cortex (AC) bouton proportions.

		Brain mass	AC large bouton %	AC small bouton %	AC cortical thickness	AC neuron density	AC glial density	AC glial: neuron ratio	AC bouton density
Brain mass	Correlation	1	0.112	−0.112	0.762**	−0.307	−0.031	0.54	−0.421
	P value		0.728	0.728	0.004	0.331	0.923	0.07	0.173
AC large bouton %	Correlation	0.112	1	−1.000**	−0.031	0.354	0.454	−0.157	0.154
	P value	0.728		0	0.924	0.259	0.138	0.627	0.633
AC small bouton %	Correlation	−0.112	−1.000**	1	0.031	−0.354	−0.454	0.157	−0.154
	P value	0.728	0		0.924	0.259	0.138	0.627	0.633
AC cortical thickness	Correlation	0.762**	−0.031	0.031	1	−0.135	0.187	0.468	−0.760**
	P value	0.004	0.924	0.924		0.675	0.56	0.125	0.004
AC neuron density	Correlation	−0.307	0.354	−0.354	−0.135	1	0.504	−0.800**	0.157
	P value	0.331	0.259	0.259	0.675		0.095	0.002	0.625
AC glial density	Correlation	−0.031	0.454	−0.454	0.187	0.504	1	0.043	−0.143
	P value	0.923	0.138	0.138	0.56	0.095		0.895	0.658
AC glial:neuron ratio	Correlation	0.54	−0.157	0.157	0.468	−0.800**	0.043	1	−0.44
	P value	0.07	0.627	0.627	0.125	0.002	0.895		0.153
AC bouton density	Correlation	−0.421	0.154	−0.154	−0.760**	0.157	−0.143	−0.44	1
	P value	0.173	0.633	0.633	0.004	0.625	0.658	0.153	

** Correlation is significant at the 0.01 level (2-tailed).

J Chem Neuroanat. Author manuscript; available in PMC 2021 December 23.

Table 8

Matrix showing the results of bivariate correlation analysis for the occipital cortex (OC) bouton proportions.

		Brain mass	OC large bouton %	OC small bouton %	OC cortical thickness	OC neuron density	OC glial density	OC glial: neuron ratio	OC bouton density
Brain mass	Correlation	1	0.301	−0.301	0.630*	−0.25	0.203	0.566	−0.454
	P value		0.342	0.342	0.028	0.434	0.526	0.055	0.138
OC large bouton %	Correlation	0.301	1	−1.000**	0.107	−0.152	0.089	0.27	0.531
	P value	0.342		0	0.74	0.637	0.784	0.396	0.076
OC small bouton %	Correlation	−0.301	−1.000**	1	−0.107	0.152	−0.089	−0.27	−0.531
	P value	0.342	0		0.74	0.637	0.784	0.396	0.076
OC cortical thickness	Correlation	0.630*	0.107	−0.107	1	0.128	−0.086	−0.056	−0.571
	P value	0.028	0.74	0.74		0.692	0.79	0.864	0.052
OC neuron density	Correlation	−0.25	−0.152	0.152	0.128	1	0.477	−0.668*	−0.086
	P value	0.434	0.637	0.637	0.692		0.117	0.018	0.791
OC glial density	Correlation	0.203	0.089	−0.089	−0.086	0.477	1	0.284	−0.159
	P value	0.526	0.784	0.784	0.79	0.117		0.371	0.622
OC glial:neuron ratio	Correlation	0.566	0.27	−0.27	−0.056	−0.668*	0.284	1	−0.062
	P value	0.055	0.396	0.396	0.864	0.018	0.371		0.848
OC bouton density	Correlation	−0.454	0.531	−0.531	−0.571	−0.086	−0.159	−0.062	1
	P value	0.138	0.076	0.076	0.052	0.791	0.622	0.848	

*Correlation is significant at the 0.05 level (2-tailed).

**Correlation is significant at the 0.01 level (2-tailed).